THE STONE OF DESTINY

CONDITION ASSESSMENT, SCIENTIFIC ANALYSIS AND DIGITAL DOCUMENTATION 2023

HISTORIC ENVIRONMENT SCOTLAND | ÀRAINNEACHD EACHDRAIDHEIL ALBA

This publication is published by Historic Environment Scotland, the lead public body established to investigate, care for and promote Scotland's historic environment. It is available digitally and free to download from the Historic Environment Scotland website:

www.historicenvironment.scot

All images unless otherwise noted are by Historic Environment Scotland.

This publication should be quoted as: The Stone of Destiny: Condition assessment, scientific analysis and digital documentation 2023 © Historic Environment Scotland 2024.

Authors: Dr Callum Graham, Reed Hudson, David Vacas Madrid, Olga Marzantowicz, Colin Muir, Dr Maureen Young.

Editor: Dr Jen Farquharson.

Cover image: The Stone of Destiny on display at its new location in Perth Museum © Historic Environment Scotland.

If you have any comments or queries about this publication please get in touch by email at technicaleducation@hes.scot

Any enquiries regarding this document should be sent to:

Historic Environment Scotland
Longmore House
Salisbury Place
Edinburgh
EH9 1SH
+44 (0) 131 668 8600

www.historicenvironment.scot

CONTENTS

Acknowledgements 1

Introduction 2

Condition assessment 3

Reed Hudson, Olga Marzantowicz, Colin Muir

- Background 3
- Methodology 3
- Condition observations 3
- Remedial treatments 38
- Conclusions and recommendations 41

Scientific investigation 44

Dr Callum Graham, Dr Maureen Young

- Notes regarding previous investigations 44
- Methodology 44
- Results 49
- Conclusions 67

Digital documentation 70

David Vacas Madrid

- Introduction 70
- 3D digitisation 70
- Pre-processing 72
- Processing 76
- Post-processing 79
- Outputs 81
- Conclusions 83

Report conclusions 84

Glossary 85

Further reading 88

ACKNOWLEDGEMENTS

Historic Environment Scotland would like to thank the following for their support in the development of this technical report:

The Commissioners for the Safeguarding of the Regalia.

Perth Museum.

Historic Environment Scotland

Ross Irving, Collections Registrar.

Kathy Richmond, Head of Collections and Applied Conservation.

Clara Molina Sanchez, Head of Applied Conservation.

Dr Nicki Scott, Senior Cultural Significance Advisor.

Dr Aurélie Turmel, Heritage Science Manager.

Dr Lyn Wilson, Head of Research and Climate Change.

INTRODUCTION

The Stone of Destiny, also known as the Stone of Scone, is one of the most precious and important icons of Scottish nationhood. It was on this stone that kings of the Scots, up to and including John Balliol in 1292, were seated at Scone when made kings, and it later served the same function for coronations of monarchs of England and of the United Kingdom in Westminster Abbey. It is a piece of sandstone quarried in the locality of Scone, and measures about 670mm by 420mm by 265mm. It has iron fittings at both ends and its wear patterns, tooling, and breaks bear witness to a long and complicated history.

The Stone was removed from Scotland by King Edward I of England soon after his subjection of the Scots in 1296. It was lodged in a chair built for the purpose, now known as the Coronation Chair, in the chapel of St Edward the Confessor in Westminster Abbey. In 1996 Queen Elizabeth II consented to the Stone being returned to Scotland, where it was displayed in Edinburgh Castle. It was housed in the Crown Room with the Honours of Scotland.

In 2020 the Commissioners for the Safeguarding of the Regalia concluded that the Stone should be the centrepiece of the new Perth Museum being developed in Perth City Hall, which opened in March 2024.[1]

In preparation for the coronation of King Charles III in 2023, the Stone was moved from Edinburgh Castle to Westminster Abbey. Before its move, a condition assessment was undertaken by specialist conservators from Historic Environment Scotland (HES) to ensure the Stone was in good condition and could be safely transported. This was also a valuable opportunity to gain a better understanding of the Stone, using innovative methodologies and technology to investigate it.

This report presents the work of three HES teams:

- a condition assessment carried out by specialist stone conservators.
- a scientific investigation by specialist heritage scientists.
- 3D digitisation undertaken by digital documentation specialists.

It outlines the discoveries made by these new investigations, why such measures are important for the future of the Stone, and the essential role of modern technology in conserving Scotland’s heritage.

1 This introduction was adapted from the 2024 Statement of Significance for the Stone of Destiny.

CONDITION ASSESSMENT

Background

A condition assessment was carried out in January 2023 as part of the preparations for King Charles III's coronation ceremony, which took place on Saturday 6 May 2023. This assessment ensured we were able to safely transport the Stone of Destiny to Westminster Abbey and install it within the Coronation Chair.

The assessment was conducted by senior stone conservators Colin Muir and Olga Marzantowicz of our Applied Conservation Unit at HES.

This was a rare opportunity for extended access to the Stone to carry out investigative analyses and record its surfaces in detail. These activities, undertaken by the Heritage Science and Digital Documentation teams respectively, are detailed later in this report. The Applied Conservation Unit undertook all movements of the Stone that were necessary for these teams to access its various sides.

Methodology

The condition assessment review focused on detecting any changes to the condition of the Stone of Destiny since its last detailed assessment in 2016, and assessing the following features of the Stone:

- **Its structural stability,** concentrating on existent cracks, fragile metal elements, and previous repairs to the fracture caused in 1950–51.
- **Its surface condition,** concentrating on visible staining, residues or various substances, and **weathered** areas vulnerable to disintegration.
- **Any new interesting features** from a historical, technological, or geological point of view.

Each face of the Stone was assessed, starting from top to bottom. The stone surface and its features were observed in both daylight and artifical light, with the naked eye and a portable microscope. The stone surface was also examined under UV light.

The current condition of the Stone was compared with its condition in 2016,[1] relying on the available photos and description.

Metal elements including iron rings, links, staples, and lead fill, were assessed separately by senior metals conservator Reed Hudson.

Condition observations

Note: the '**dexter**' / '**sinister**' convention is used to delineate sides and avoid confusion based on the observer's viewpoint. This system is widely used in conservation and originates in heraldic notation. Where an object has a 'front' face, the sides dexter (right) and sinister (left) are from the object's 'viewpoint' facing forward.

When describing locations within a given face, ‘left’ and ‘right’ have been used as the viewer is looking at it (eg ‘the lower left of dexter face’). These descriptions assume the Stone is sitting conventionally on its base (the underside. See Fig 1).

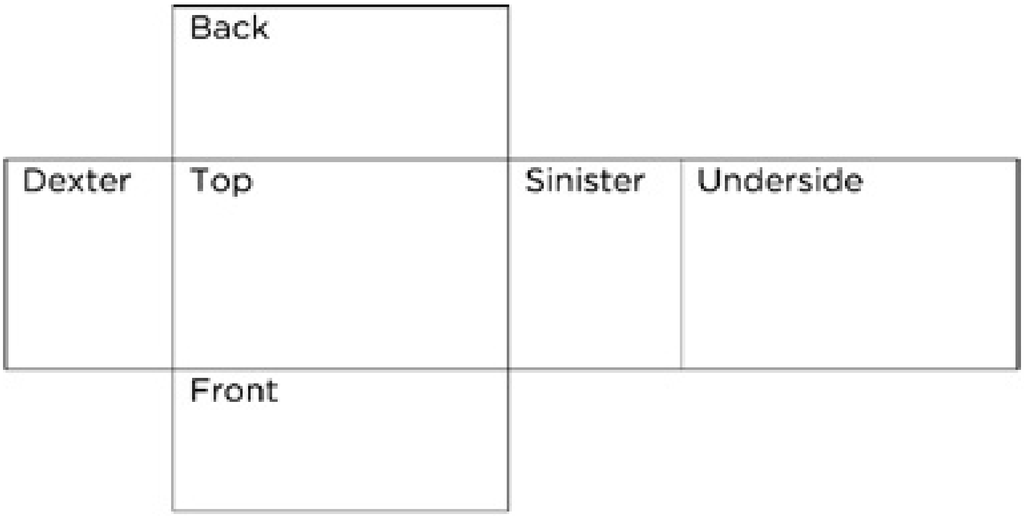

Fig 1. A diagram illustrating the locations of the faces of the Stone of Destiny.

Top face of the Stone of Destiny

The condition of the top surface is stable (Figs 2–6). There are no signs of any active disintegration (Fig 2) nor any new **iron oxide** spots, which is to be expected as the Stone has been displayed in a controlled and stable environment.

The staining in the circular sockets for the iron rings, already noted in 2016, has neither expanded nor intensified, suggesting that there is no active corrosion happening to the iron elements (Figs 7–10).

No expansion or intensification of the dark staining covering much of the central part of the upper face has been observed since it was photographed in 1996 (Figs 5 and 6).[2] It was thought that the staining might relate to the Stone’s previous location at Westminster Abbey or was due to its possible burial during the Second World War.[3] Recent scientific analysis has shown the dark stained area is richer in zinc. The source of the zinc is not known.[4] It may have been through direct contact with a metallic object or from absorption of a zinc-contaminated solution, even in a burial scenario. As a result, the staining may still be related to the burial of the larger section in ‘open country’,[5] as the staining is only noticeable in the larger fragment of fractured stone.

Additionally, the area was observed under UV light, revealing staining of a different nature, which is visible in daylight when looking at the stone surface from an angle (Figs 11 and 12). The staining forms a shiny streak and a spot. The origin of this is unknown. However, staining of a similar shape and in a similar location can be seen on a photo of the Stone from the past (dated latest 2012). The staining visible on this older photograph resembles a drip from melted wax or silicone (Fig 13).

Fig 2. General photo of the top face of the Stone (2023).

Fig 3. Close up photo of the top face (2016).

Fig 4. Same area as seen in Fig 3, photographed in 2023.

Fig 5. The top surface with a noticeable fine crack and dark staining in the middle of the Stone, photographed in 2016.

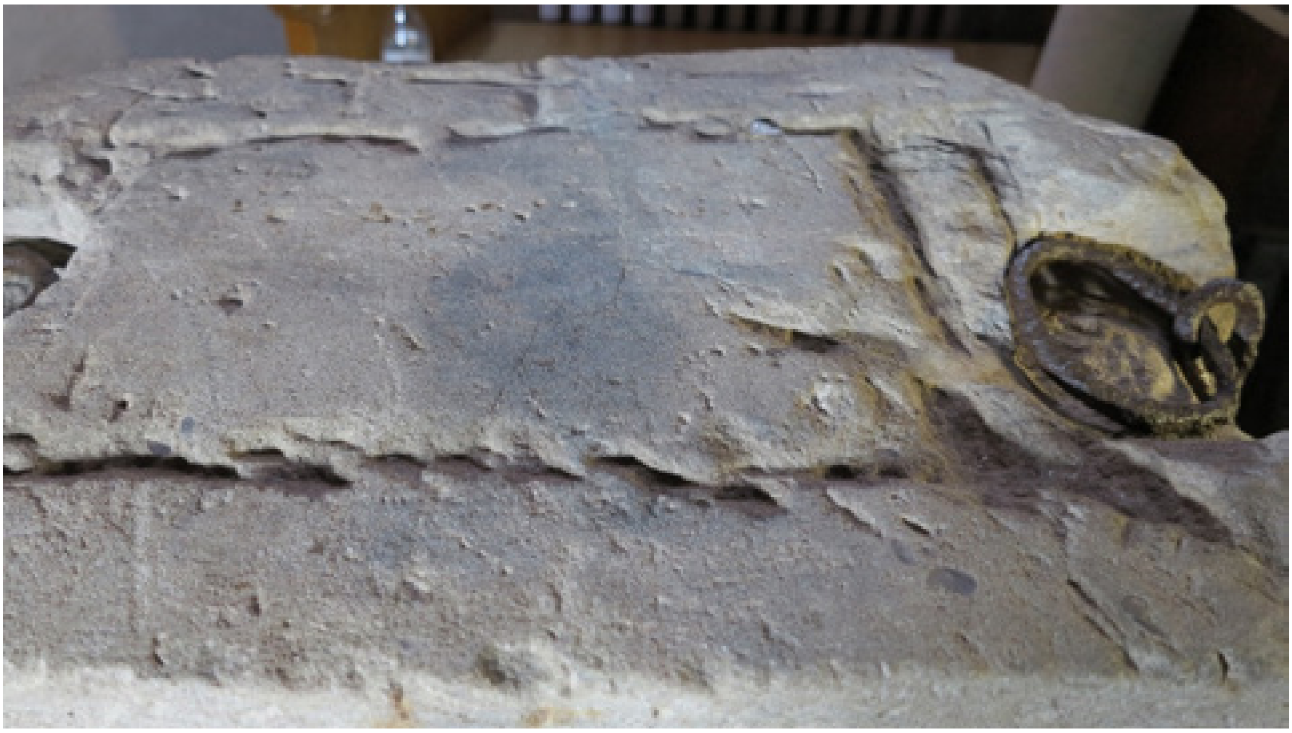

Fig 6. The same area as seen in Fig 5, recorded in 2023.

Fig 7. Dexter face socket (2016).

Fig 8. Dexter face socket (2023).

Fig 9. Sinister face socket (2016).

Fig 10. Sinister face socket (2023).

Fig 11. Newly identified staining under UV light (2023).

Fig 12. The same area in daylight (2023).

Fig 13. Staining identified on the Stone's top surface in 2023 and already visible on an older photo of the Stone from no later than 2012.

The condition assessment also identified areas with old hairline cracks in pointing repairs from the 1950s (see Figs 3 and 4), which are stable, have not expanded and do not appear to be opening up. Through condition checks like this one, these areas will continue to be monitored for any changes, which could indicate structural movement or failure of the internal fixings.

A hairline fissure, extending from the joint corner in the centre of the top surface towards the front edge, is similarly stable (Fig 14). It is possible that an inherent geological weakness in the Stone (a fissure or 'dry') determined the way the Stone has broken in the past. Some sources reveal that there was a crack already visible in photographs dated pre-1950, which would confirm this hypothesis.[6] This feature of the Stone should be monitored closely.

A watercolour wash applied to the repair in 1996 is still serving its function to disguise the previously applied cement mortar (1950). Traces of the mortar located in the dexter socket do not show any changes.

Fig 14. Close-up of a hairline fissure (2023).

At the time of the condition assessment, the top surface was covered with white elongated flecks of what looked like a waxy substance, similar to silicone sealant (Fig 15). These flecks don't seem to have adhered to or affected the stone surface, and they were removed with a soft, dry brush. Although unconfirmed as the cause, a review of the silicon rubber seals in the glass display case was undertaken to check for any deterioration that may require their renewal.

The **cementitious** repair applied to the Stone in 1950–51 contains fibrous material, which glowed under UV light.[7] This could be identified under a portable microscope as small pieces of wood or brush bristles; probably used to finish or work over the applied repair (Figs 15–17).

Fig 15. The circled area (top) shows a repair joint with visible fibrous material incorporated into mortar (2023). The area indicated by an arrow (left) shows visible white flecks of a silicone-like substance deposited on the stone surface.

Fig 16. Close-up of the area with visible fibrous material within the cementitious repair (2023).

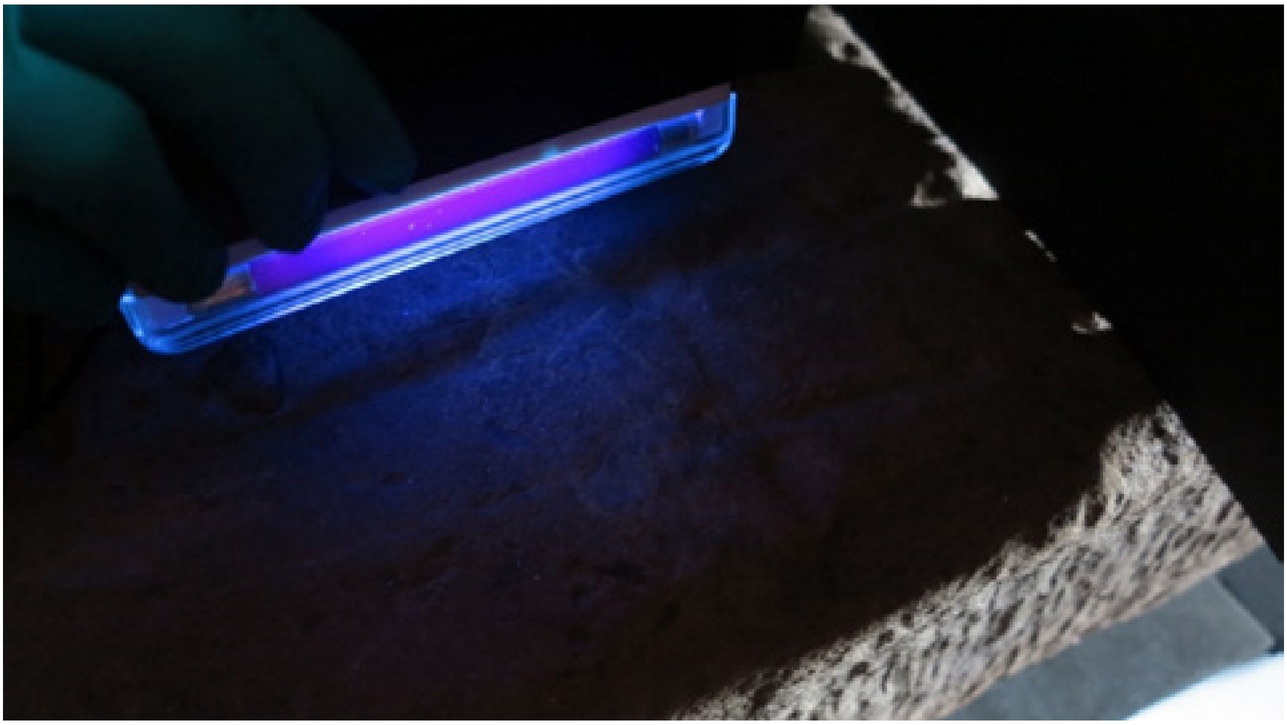

Fig 17. The same area as Fig 16 under UV light. Note the slightly glowing visible line.

Front face of the Stone of Destiny

The front face surface appears to be stable. None of the features already identified in 2016 showed any changes, including:

- iron staining.
- shiny surface **accretion** in the low area of the front face (which seems to be greasy in nature and attracts cloth and paper fibres).
- minute blue paint traces (most likely from tools used for movement at some point during the 20th century) (Fig 18).

A small, resinous, semi–transparent yellow-white residue was spotted on the lower left corner of the front face (Fig 19). It was also visible as a glowing spot under UV light (Fig 20). The nature and location of the residue may suggest a **deposit** of substances used for decorating or protecting the wooden Coronation Chair (eg varnish), which could have been grazed during previous de-installations of the Stone from the chair. Westminster conservators informed the team of the presence of ‘orpiment’, a hazardous substance previously used on the chair that required PPE and risk management procedures when handling. The potential for this substance leaving residue on the Stone should be considered not only for condition assessment and conservation purposes, but for health and safety reasons for any future interactions with the Stone.

The condition assessment was able to identify areas that required attention to ensure the good condition of the Stone. This included a fine fissure and a flake slightly separating from the underside of the front face, which was noticed during the check (Fig 21), and could therefore be addressed in the next phase of conservation work (see the Remedial Treatments section of this condition assessment report for more details).

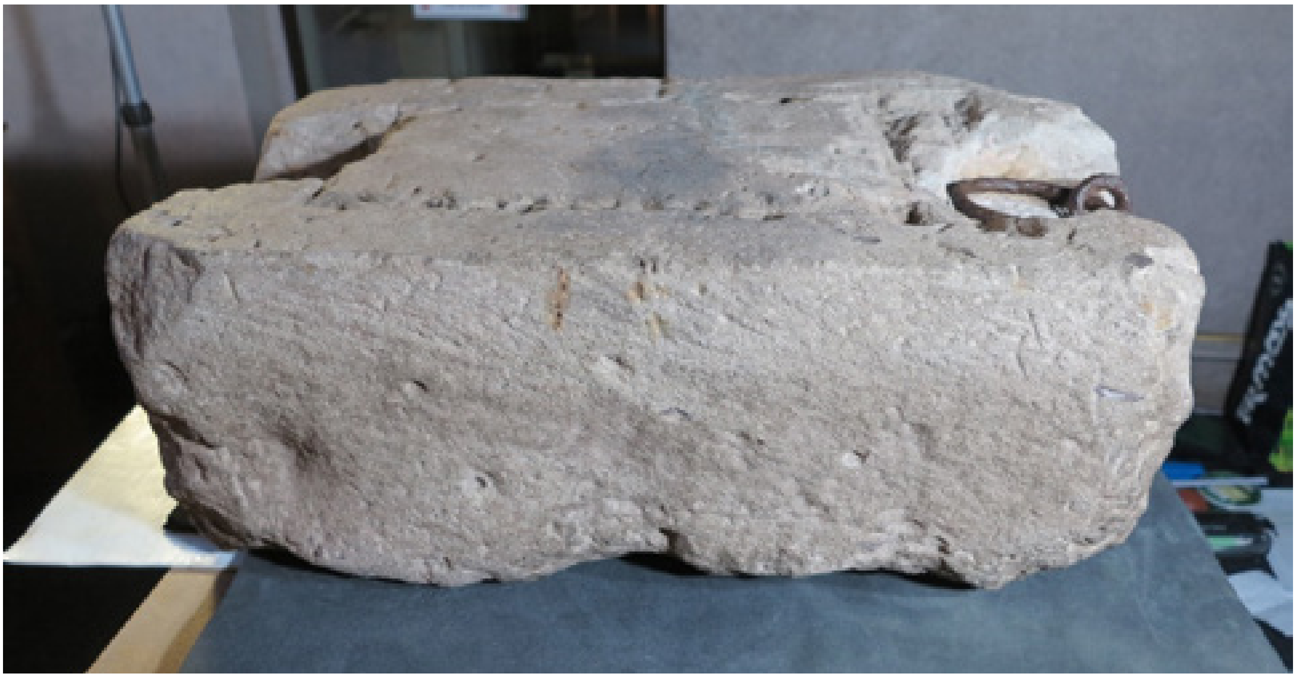

Fig 18. General photo of the front face (2023).

Fig 19. Lower left corner of the front face (2023).

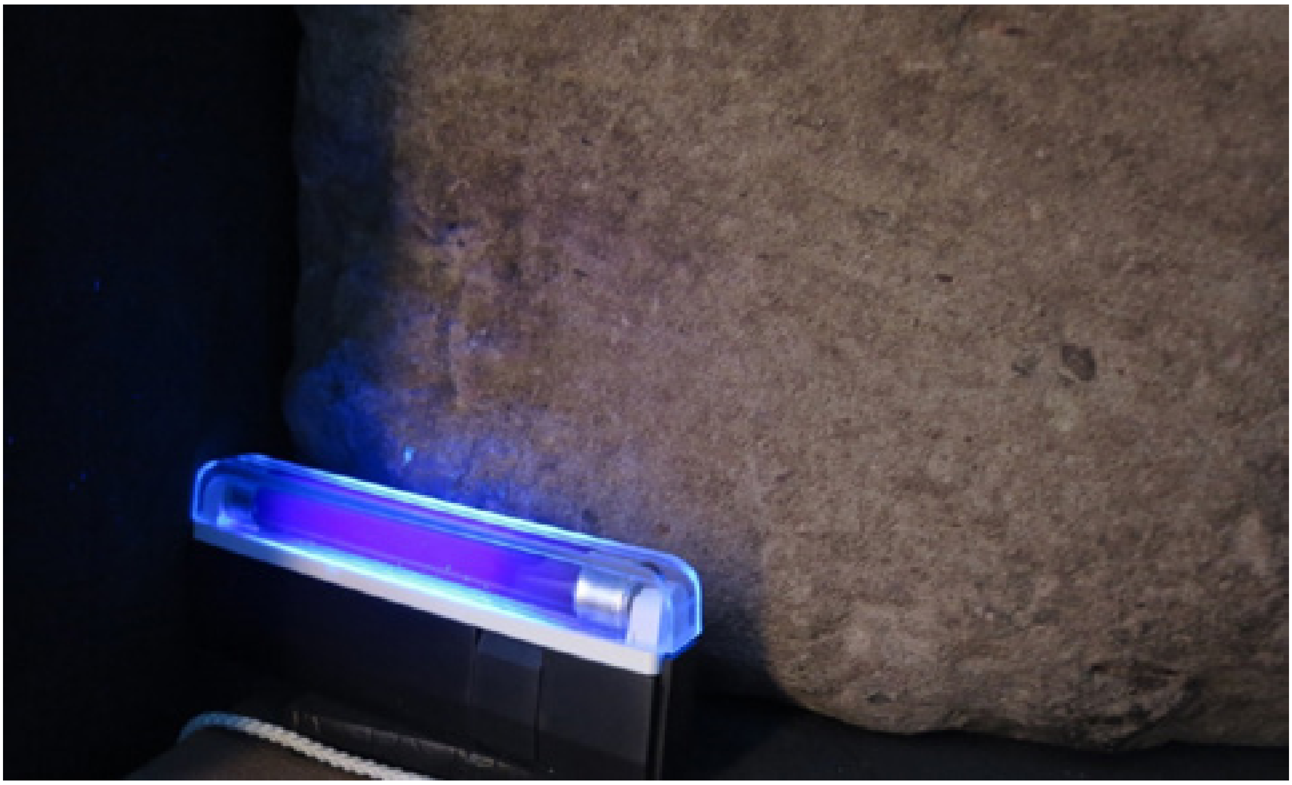

Fig 20. Lower left corner of the front face. The resinous residue visible in UV light (2023).

Fig 21. Lower edge of the front face. Visible fine fissure and a stone flake (2023).

Back face of the Stone of Destiny

The condition of the back surface is stable (Fig 22). Traces of mineral adherences, most probably **gypsum**,[8] do not show any changes and seem to be intact (Figs 25 and 26).

The cementitious pointing applied around the 1950 repair joint in this location does not show any signs of dislodging, and the fine cracks noted in 2016 have neither expanded nor opened up (Figs 23 and 24).

Fig 22. General view of the back face (2023).

Fig 23. Condition of the joint over the repair (2016).

Fig 24. The same area as in Fig 23, photographed in 2023.

Fig 25. Photo record of the mineral mortar residue (2016).

Fig 26. The same area as in Fig 25, photographed in 2023, with no discernible change.

A hole repair, found in 1996 and filled with an **acrylic** mortar, was slightly off the colour of the Stone and required replacement (Figs 27 and 28). The drilled hole had previously held a small lead tube containing an offcut from a 1970s authentication document (accession no. E6120) and had been covered with a wax seal.

The edges of the hole repair also showed fluorescence in UV light. The thread-like appearance of the glowing substance indicated the presence of some fibres, perhaps gauze or paper, most probably used during repairs (Fig 29).

One area of a scratched white inclusion in the Stone glowed under UV light, suggesting the presence of a mineral inherent to the Stone fluorescing in UV, or traces of substance glowing in the UV (Fig 29).

Fig 27. Visible acrylic mortar-fill not matching the stone colour anymore and requiring replacing (2016).

Fig 28. The same area as Fig. 27 after the replacement of the fill in 2023.

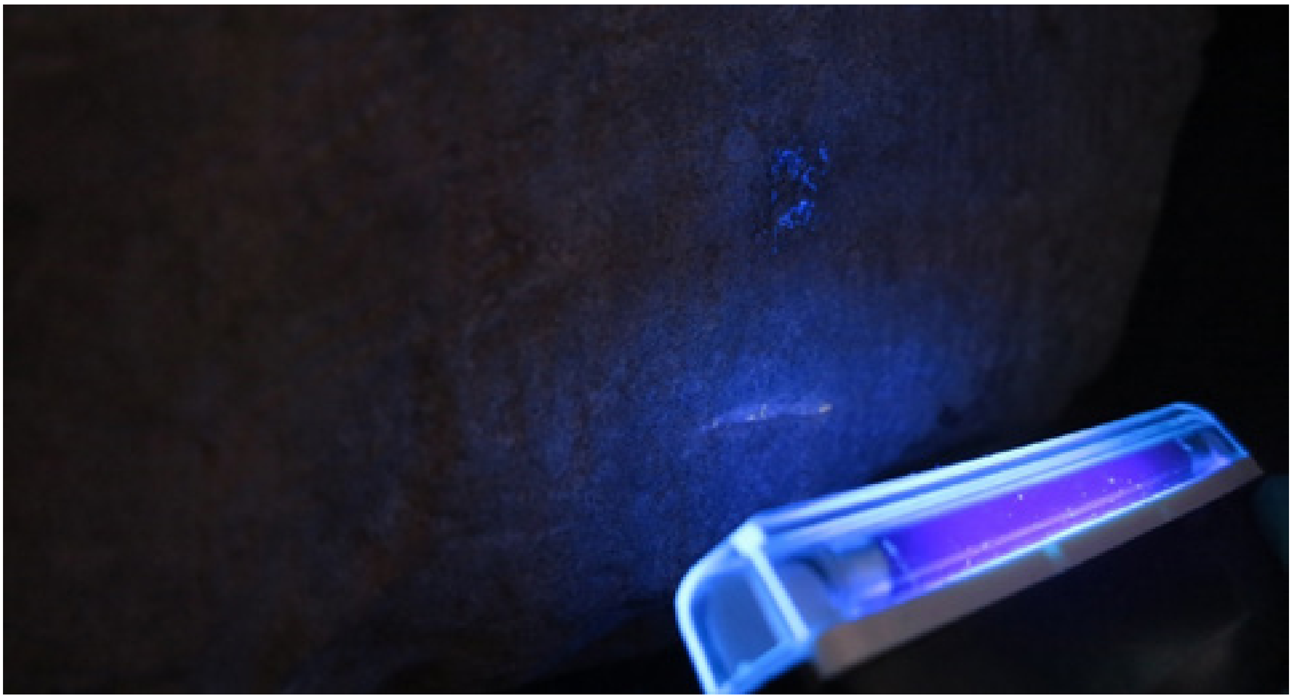

Fig 29. Lower right corner of the back face under UV light (2023).

Bottom face of the Stone of Destiny

The surface of the underside of the Stone has a slightly rougher texture and may be more prone to disintegration than the Stone's other faces.

The rust staining already noted in 2016, and probably related to the presence of the two transverse supportive iron bars added to the chair construction in 1821,[9] has not intensified or expanded (Figs 30 and 31).

The condition of the mortar in the repaired joints is stable, as the partial cracking along its edge noted in 2016 does not show any signs of expansion in any direction.

Fig 30. General view of the bottom face, with the Stone laid on the back face (2016).

Fig 31. General view of the bottom face, with the Stone laid on the front face (2023).

Near the edge, between the bottom face and the back face, a previously undocumented earlier incised inscription has been noticed. The sharply incised inscription represents Roman numbers or letters: XXXV or XXXVX,[10] with the last X being slightly shallower (Figs 32a, b and c). The inscription appears to be relatively modern, possibly 20th century, and though there is no record of its purpose, it is conceivable that the marking may have been added to help identify the Stone or a part of it. The two occasions which seem most likely are: (1) during the Second World War when the Stone is thought to have been concealed for its safekeeping, or (2) in the 1970s when concerns were heightened following a second (failed) attempt to remove the Stone from Westminster Abbey. The visible number could possibly be part of an **accession system**.

Fig 32a. Close-up of the incised numbers/letters.

Fig 32b. Close-up of the incised numbers/letters (macro image).

Fig 32c. Close-up of the incised numbers. Macro photo modified on Photoshop to extract the lines (2023). Figs 32b and 32c provided by the Digital Documentation Team.

Sinister end face of the Stone of Destiny

The condition of the surface of the sinister end face is stable (Figs 34 and 35). No significant signs of any active disintegration have been observed, and the reversible colour wash still serves its function to disguise inexpertly applied mortar over the repair joint.

However, the condition assessment also found some areas on the face that will require continued monitoring to keep the Stone in good condition, including: a fine diagonal crack radiating from the lead plug towards the repair joint; a noticeable area slightly prone to flaking under the lead plug (Fig 36); and a fine crack in the repair area located in the socket for the metal elements (Fig 37).

Three areas on the Stone's face showed fluorescence under the UV light (Fig 38). Two of them (top) were of a resinous residue and the one below appeared to be a mineral inherent to the Stone.

Fig 33. Sinisted end face of the Stone of Destiny with iron ring extended and supported (2016).

Fig 34. General photo showing the ring and link lowered on the soft padding (2023).

Fig 35. General photo showing the ring and link rested in the socket (2023).

Fig 36. The sinister end face showing a visible fine crack and the area prone to flaking (2023).

Fig 37. The repair area in the socket for the metal elements (2023).

Fig 38. The sinister end face under UV light and the three fluorescing areas visible (2023).

Dexter end face of Stone of Destiny

The condition of the surface of the dexter end of the Stone is stable (Fig 40). The iron staining, already identified in 2016, caused by the corrosion of iron elements located in the socket dedicated to them has neither intensified nor expanded (Figs 39 and 41). Similar observations were made of the iron staining inherent to the Stone and present on the right lower corner of the left end face (Figs 42 and 43).

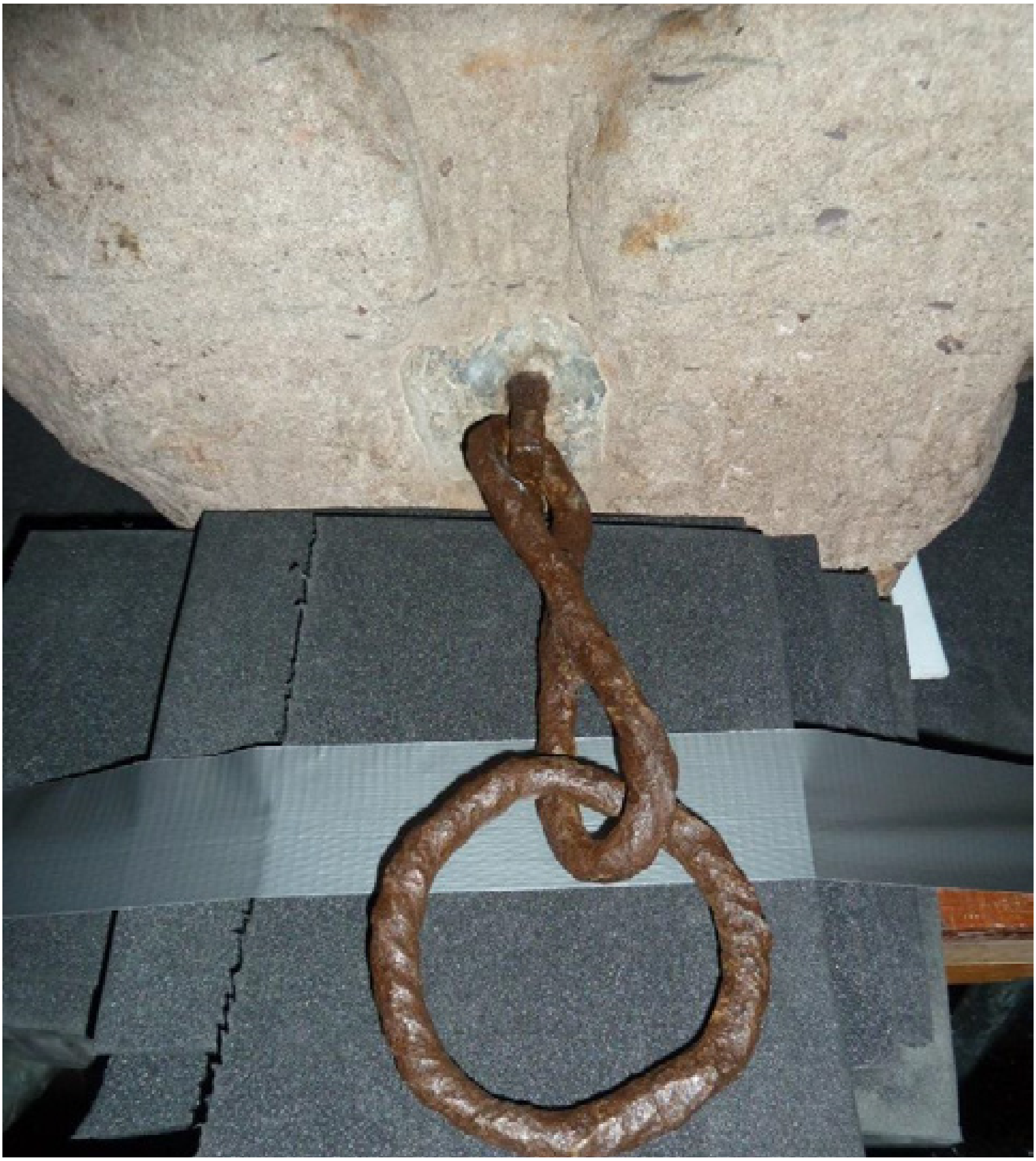

Fig 39. General photo of the dexter end face (2016).

Fig 40. General photo of the dexter end face (2023).

Fig 41. Visible staining in the socket for the iron ring (2023).

Fig 42. Visible iron staining inherent to the Stone and residues of the brown matter (2016).

Fig 43. Same area as Fig 42, photographed in 2023.

The resinous, semi-transparent yellow-brown substance is most probably organic, deposited onto the area under the two lines incised on the left top corner of the left end face. It was observed under UV light (Figs 44-46). The residue showed fluorescence of similar colour and intensity as the deposit on the left lower corner of the front face of the Stone (Fig 20).

In addition to the observations from 2016, an area of scratched or incised pattern was identified during the recent assessment (Fig 47). It is located in the lower right corner and the pattern resembles a letter H.

Fig 44. Two visible carved/incised lines, and below, a brown substance of organic nature (2016).

Fig 45. The same area as Fig 44, photographed in 2023.

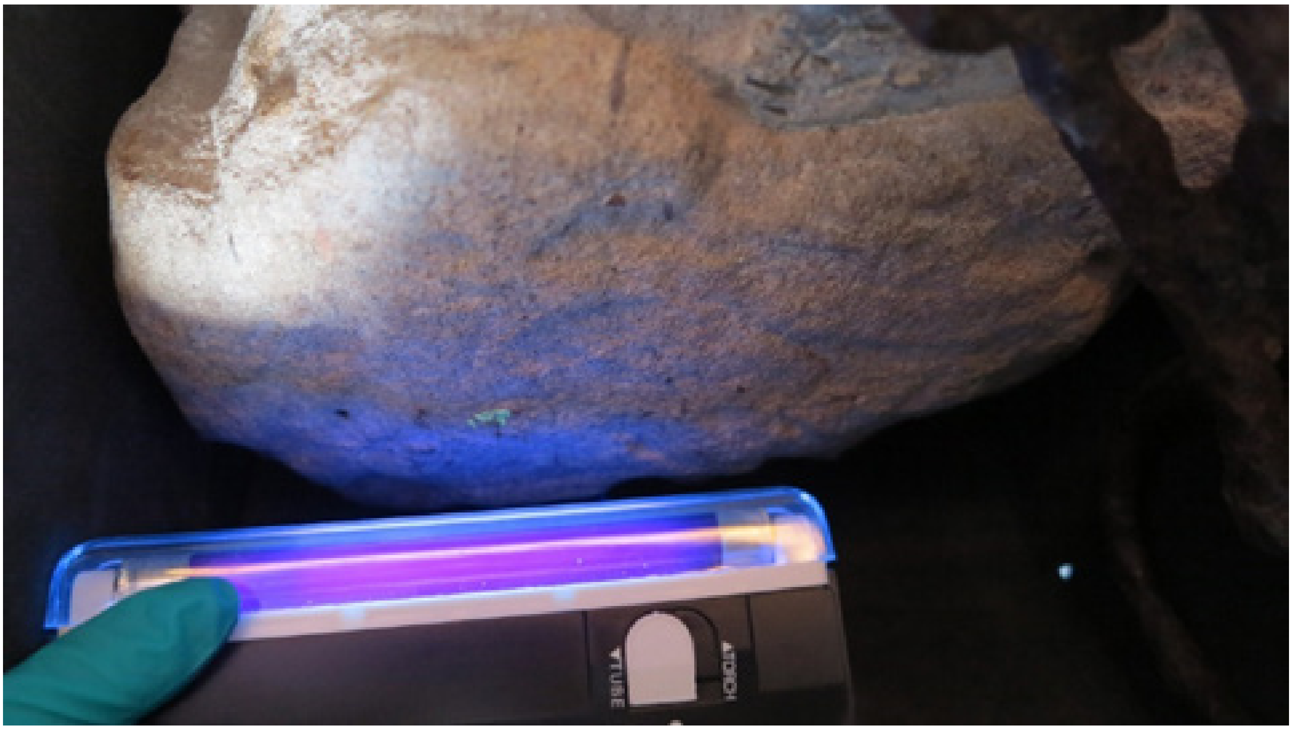

Fig 46. The same area as in Figs 44 and 45, observed under UV light.

Fig 47. Incised pattern resembling letter H.

Metal elements

Metal elements of the Stone of Destiny were briefly assessed by stone conservators from our Applied Conservation Unit during the condition check. This was followed by a more detailed assessment of the metalwork conducted by the team's senior metals conservator, Reed Hudson.

The visible metalwork of the Stone consists of a pair of **articulated** iron rings joined to staples in the Stone via a pair of forge-welded, figure-eight links. These are dimensionally designed to fold into the carved sockets on the top of the Stone, presumably for compactness in transport or for placement in ceremonial use. All of these components are constructed from twisted wrought iron rod of a fairly consistent 11–13mm diameter.

The staples are attached to the Stone via poured lead fills into pre-prepared sockets. The staples have been cut or filed at some stage possibly to fit into the Coronation Chair, with 1mm or less of material joining them. This has left both of them extremely weakened.

There are anecdotal references to metal pins used internally to join broken fragments of the Stone in 1950–51. This was duly confirmed by X-ray photography in 1996. As these pins are not physically accessible, their material, precise dimensions and condition are presently unknown.

The iron elements did not show any significant signs of active corrosion. A transparent coating has been applied at some point in the past. However, the condition assessment identified a few areas of a matte orange iron oxide, indicating that the coating has started to fail (Fig 51). This was addressed during the subsequent remedial conservation (see the Remedial Treatments section of this condition assessment report).

The condition assessment also revealed small areas of flaking iron corrosion and a previously undocumented crack in the staple on the dexter side of the Stone. Overall, the fragile nature of the iron staples makes them the most vulnerable to damage of all elements of the Stone. In case of any examination or movement of the Stone, these must be carefully protected (Figs 49 and 51).

The lead fill around the staples appears stable, but showed tendencies to powdering in places, which may be linked to an acidic environment in the display case due to the wood used in its construction (Fig 49). These areas were consolidated as part of the remedial conservation work. They should be carefully monitored and addressed by an experienced metal conservator if they change.

Fig 48. Ironwork and lead plug located on the sinister face (2023).

Fig 49. Close-up of the sinister face showing the thinness of the staple and its fragility and vulnerability to mechanical damage (2023).

Fig 50. Ironwork and lead plug located on the right (dexter) face (2023).

Fig 51. Close-up of the dexter face showing the fragility of the ironwork and its vulnerability to mechanical damage (2023).

Remedial treatments

The Stone

A few areas of the Stone of Destiny were identified as ones which would benefit from non-invasive intervention and were treated. The treatments ensured the stability of the Stone during its transport and future display, as well as improving its visual presentation.

1. The fine crack on the top of the Stone was injected with a 2.5% solution of Paraloid B-72 acrylic resin in acetone/IMS (50/50) (Fig 14).

2. The fine crack and area slightly prone to flaking near the lead fixing in the sinister end face of the Stone were injected with 2.5% of B-72 in acetone/IMS (50/50) as well as filled and edge-pointed with acrylic-based mortar repair (5% B-72 in acetone/IMS mixed with a stone dust and sand) (Figs 52 and 53).

3. The open crack above the stone flake in the lower edge of the front face was injected with 2.5% B-72 in acetone/IMS (50/50) (Fig 21).

4. The acrylic mortar used to fill the drilled hole was dissolved with an application of acetone in a syringe, then removed. The hole, which still contains the empty lead container, was then deep-filled with a properly colour-matched fill of the same material at 5% B-72 in acetone/IMS (50/50) (Figs 27 and 28).

Fig 52. Fine crack and area slightly prone to flaking in the right (sinister) face before any treatments.

Fig 53. The same area shown in Fig 52 after injection and filling with acrylic resin mortar repairs.

Metal elements

In March 2023, areas of powdering on the lead fills were consolidated with two applications of 10% w/v B-72 in acetone. The first coating was allowed to dry overnight to judge the potential effects of saturation and shine. When the appearance was deemed acceptable a second coating was applied to select areas where powdering was still visible.

Given the complexity of moving the Stone, the treatment of the remaining metalwork was completed with the Stone in situ in its new long-term location at Perth Museum.

The conservation treatment proceeded as follows:

1. The ironwork elements were cleaned by brushing a solvent mixture (50/50 mix of acetone and industrial methylated spirits [IMS] determined by solvent testing) with a soft brush, then using a natural bristle brush to mobilise and remove the old coating. In fragile or hard-to-reach areas a cotton swab was used to clear the solvent. The Stone was protected at all times during this process with acid-free tissue paper and Tyvek coverings (Fig 54).

2. A thin, cohesive layer of 3% w/v Paraloid B-44 in acetone was applied to the surface of the ironwork and left to cure for 24 hours.

3. To stabilise the crack in the staple, various fill materials were trialled with different mineral pigments to ensure a good colour match with the iron (Fig 55).

The resulting fill material was composed of:

- 8g of 20% w/v Paraloid B-48N in 50/50 acetone/IMS
- 8g iron powder
- 0.6g glass microballoons
- 0.1g fumed silica
- 1g burnt umber pigment
- 1g natural umber pigment
- 0.5g terra di sienna pigment.

4. A second and final coating of 3% w/v Paraloid B 44 in acetone was then added to both sides of the ironwork. The adhesive was mixed with a small amount of fumed silica to adjust the level of shine imparted by the coating. This mixture was also applied to the lead fills to reinforce the coating applied in March 2023, deterring further lead corrosion.

Fig 54. Working set-up during the removal of the previous coating.

Fig 55. The cracked staple before (left) and after (right) application of the fill.

Conclusions and recommendations

- Limit movement of the Stone to minimum. If necessary, then the movement and handling should be conducted by qualified and trained members of staff familiar with the lifting and moving route, and the condition of the Stone itself. It is advised that a stone conservator should be present during any movement of the Stone. Another assessment should take place prior to any future moves to determine the best way of stabilising and protecting the Stone and its ironwork based on condition.
- Where possible, use lifting aids to move the Stone and reduce manual lifting. However, while using lifting aids, stabilise the Stone manually if necessary.
- Always support both edges of the Stone and secure and protect its fragile metal elements (Fig 56).
- Monitor the cracks in the repair and the hairline crack coming from the joint.
- Monitor the condition of the metal.

Fig 56. Recommended method of securing the ironwork during any movement.

Endnotes

1 This condition assessment is an addendum to the detailed condition assessment conducted in 2016 by stone conservator Christa Gerdwilker.

2 The wider expansion of the staining that took place pre-1996 may have been facilitated by the presence of a hairline fissure, extending from the joint corner in the centre of the top surface towards the front edge of the top surface, allowing moisture ingress and therefore increasing the vulnerability of the area to soiling deposition.

3 According Nick Aitchison, *Scotland's Stone of Destiny* (2009), p.119, during the Second World War, the stone was buried secretly in the Islip Chapel.

4 More information can be found in the Scientific Investigation section of this report.

5 According to S Brocklehurst, (www.bbc.co.uk/news/uk-scotland-tayside-central-63130942), the large section of the stone was buried in open country near Rochester in Kent after being removed from Westminster Abbey in 1950.

6 D. Breeze and G. Munro, *The Stone of Destiny, Symbol of Nationhood*, (Historic Scotland, Edinburgh, 1997), p. 30. W. Rodwell, *The Coronation Chair and Stone of Scone: History, Archaeology and Conservation*, (Oxbow Books, Oxford, 2013), pp. 11-12.

7 A list of ultra-violet, fluorescent materials relevant to conservation can be found at: https://aiccm.org.au/network-news/summary-ultra-violet-fluorescent-materials-relevant-conservation.

8 More information including the results of examination of traces of the mortar can be found in the Scientific Investigation section of this report.

9 W. Rodwell, *The Coronation Chair and Stone of Scone: History, Archaeology and Conservation*, (Oxbow Books, Oxford, 2013), p.153.

10 The additional 'X' at the end has been noticed on the orthoview scans included in the report conducted by the Digital Documentation Team.

SCIENTIFIC INVESTIGATION

A non-destructive analytical survey on the Stone of Destiny (Stone of Scone) was undertaken in January 2023 at Edinburgh Castle prior to its transfer to Westminster Abbey for the Coronation of King Charles III. Further analyses were carried out in November 2023.

The purpose of the survey was to improve baseline information on the Stone of Destiny to support our understanding of its history and future conservation work, by:

- performing analysis at 86 locations across the Stone;
- analysing, using **portable X-ray fluorescence** (pXRF), the chemical element composition of the Stone and contaminants on its surface, deposited through usage;
- documenting with a digital portable microscope the texture and minerals composing the Stone at locations of pXRF analysis;
- colour analysis of the Stone at locations of pXRF analysis.

Notes regarding previous investigations

The composition of the Stone of Destiny with respect to local Perthshire sandstones was previously examined by Fortey et al. (1998).[1] At that time, pXRF analysis was not available. Characterisation by Fortey et al. was carried out by comparing the texture, **petrographic analysis** and colour of the Stone of Destiny, with samples from **Lower Devonian sandstones** of the Perth and Dundee areas and masonry from Dunstaffnage Castle.

Fortey et al. suggest that the Stone of Destiny is similar to **Scone Formation sandstones** from the Lower Devonian in the Perth area and note in particular its similarity to sandstone in the vicinity of Quarrymill, near Scone Palace. They include a discussion of previous investigations regarding the composition and provenance of the Stone of Destiny. The Stone of Destiny had been described by previous investigators as '**calcareous**' (mostly or partly composed of **calcium carbonate**), which does not concur with Fortey et al's examination of a thin section from a pre-existing chip from the Stone of Destiny. They describe the composition as indicating that of a **litharenite** (a sandstone with a significant component of **lithic fragments**).

Methodology

Portable X-ray fluorescence

The portable X-ray fluorescence (pXRF) equipment used was a Bruker Tracer 5g. pXRF analysis was carried out using Bruker's GeoExploration calibration application, method 'Oxide3phase'. Analysis was carried out in air. The analysis period was 90 seconds (30 seconds each at the following three settings):

- 30 kV, 13.8 µA, Ti 25 µm + Al 300 µm filter, 8 mm collimator;
- 50 kV, 23.4 µA, Cu 75 µm + Ti 25 µm + Al 200 µm filter, 8 mm collimator;
- 15 kV, 11.55 µA, no filter, 8 mm collimator.

The GeoExploration calibration results were further processed using results from analysis of 13 powdered calibration standards,[2] to check and amend the accuracy of coefficients in the GeoExploration calibration.

Analysis was non-destructive, examining the Stone of Destiny in its current condition at 86 locations (Fig 1), including a few analyses of inclusions and obvious surface deposits.

Surfaces varied in roughness, affecting the accuracy of results. Surface roughness mainly affects data for lighter elements such as Mg, Al, Si and P (whose X-ray energy is more strongly attenuated in air). Absorption of X-ray energy in air precluded quantification of sodium (Na).

Key to elements

Ag: silver	Al: aluminium	As: arsenic	Au: gold
Ba: barium	Bi: bismuth	Ca: calcium	Cd: cadmium
Ce: cerium	Cl: chlorine	Co: cobalt	Cr: chromium
Cu: copper	Fe: iron	Ga: gallium	Hf: hafnium
Hg: mercury	K: potassium	La: lanthanum	Mg: magnesium
Mn: manganese	Mo: molybdenum	Nb: niobium	Ni: nickel
O: oxygen	P: phosphorus	Pb: lead	Pd: palladium
Pt: platinum	Rb: rubidium	Rh: rhodium	S: sulphur
Sb: antimony	Se: selenium	Si: silicon	Sn: tin
Sr: strontium	Ta: tantalum	Te: tellurium	Th: thorium
Ti: titanium	Tl: thallium	U: uranium	V: vanadium
W: tungsten	Y: yttrium	Zn: zinc	Zr: zirconium

Digital portable microscope

Microscope analysis was undertaken across all 86 locations chosen for pXRF analysis, and on additional selected locations to provide representative coverage of the Stone.

A Dino-Lite Edge AM7915MZT USB microscope attached to a Panasonic Toughpad tablet was used to obtain microscopic images at high magnification of the Stone. The microscope was calibrated using a supplied scale card prior to analysis.

In-situ non-destructive microscopic analysis provided information on the stone mineralogy and texture, particularly grain size, shape and compaction. Image post-analysis was undertaken using DinoCapture 2.0 software.

Colour analysis

Colour was assessed using a Konica Minolta CR-410 chroma meter, providing diffuse lighting from a pulsed xenon lamp over an area 53 mm in diameter using illuminant C light source. The chroma meter was calibrated against a standard white plate.

The colour space was L* a* b* where L = lightness (0-100%), a* = green-red coloration (negative values are green and positive values are red) and b* = blue-yellow coloration (negative values are blue and positive values are yellow). Higher positive and negative values indicate more intense coloration. Each location was analysed three times.

Locations of pXRF analyses

A total of 86 analyses were carried out on all six faces of the Stone of Destiny at locations shown in Figure 1.

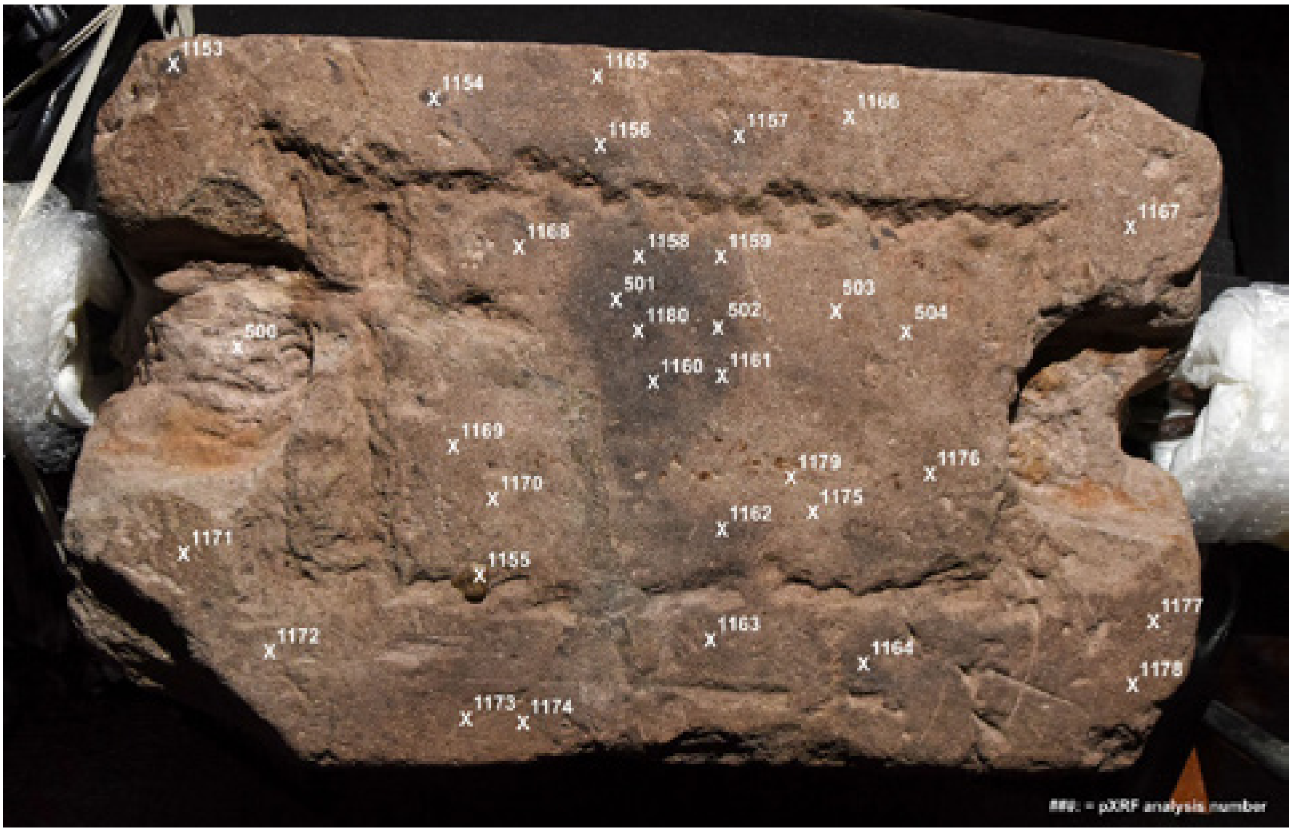

Fig 1a. Locations of pXRF analyses (8 mm diameter) on the top surface of the Stone of Destiny.

Fig 1b. Locations of pXRF analyses (8 mm diameter) on the front surface of the Stone of Destiny.

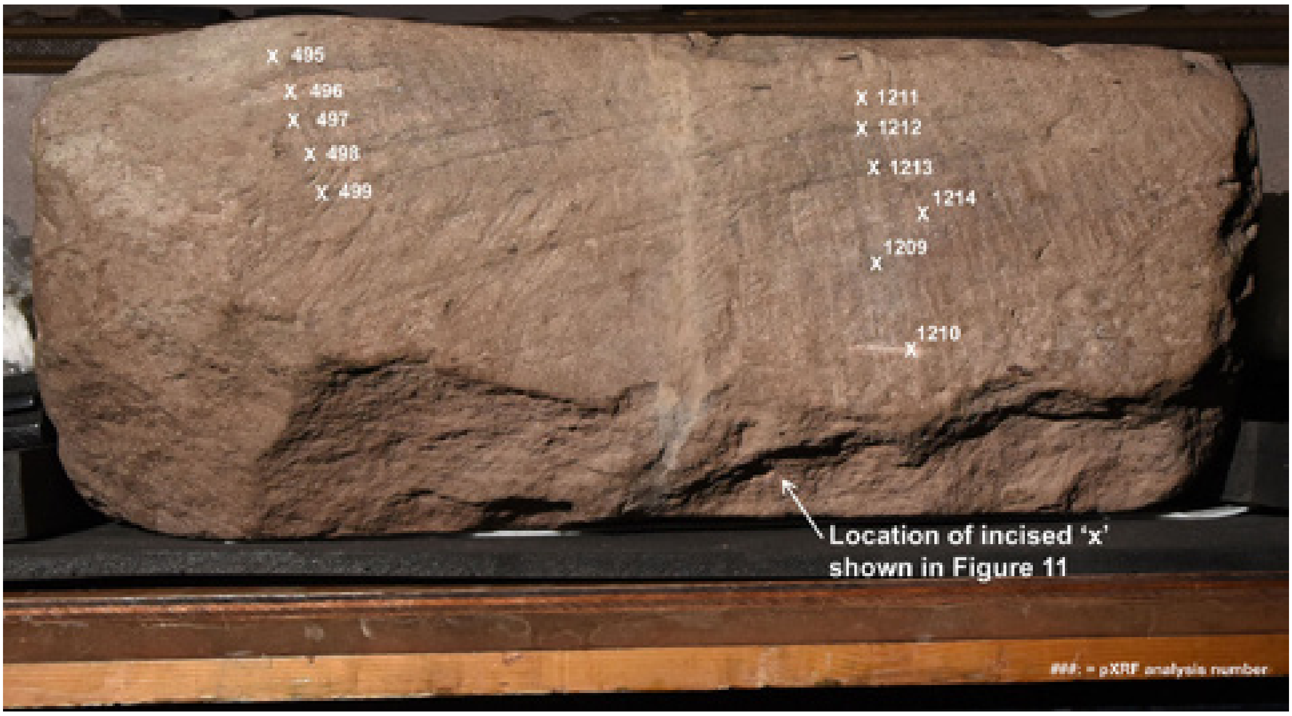

Fig 1c. Locations of pXRF analyses (8 mm diameter) on the back surface of the Stone of Destiny.

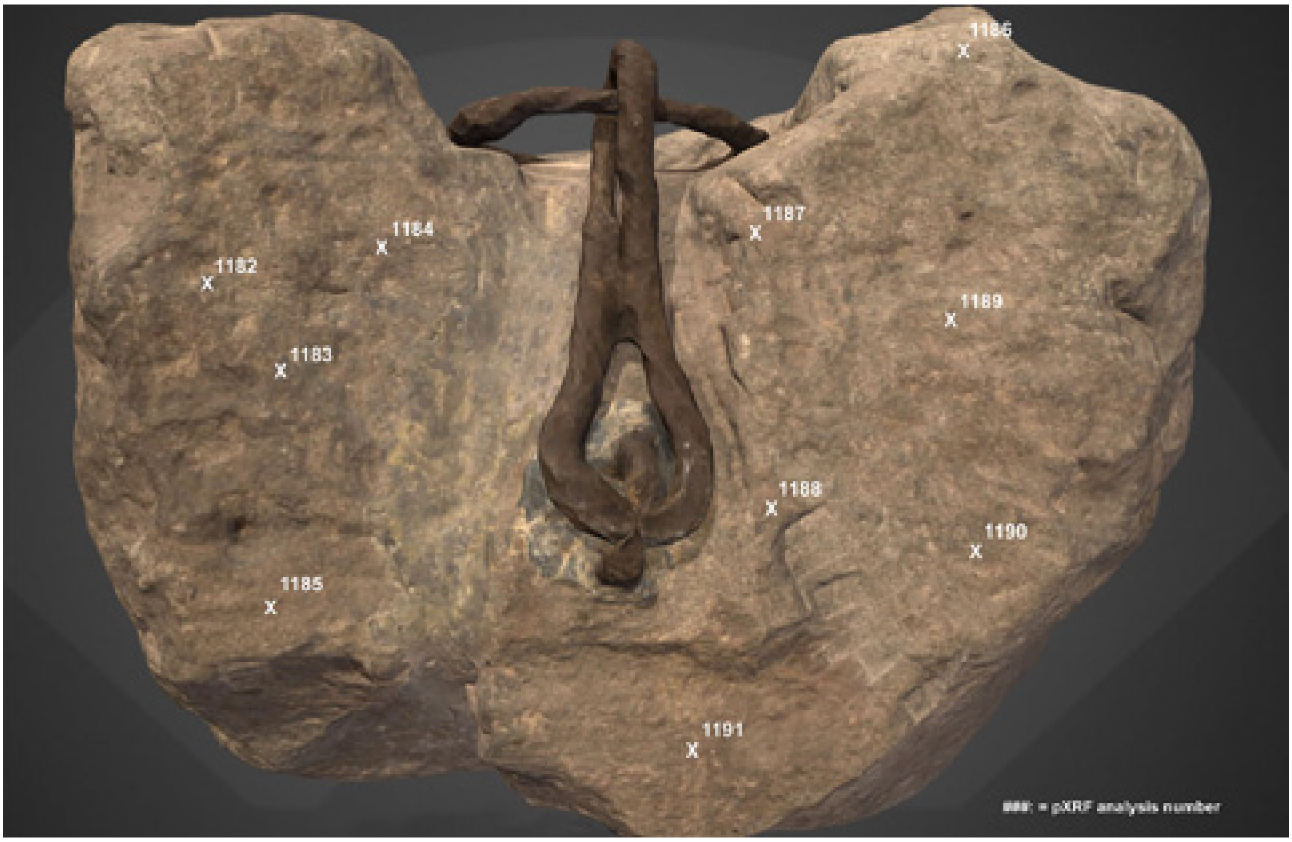

Fig 1d. Locations of pXRF analyses (8 mm diameter) on the sinister surface of the Stone of Destiny.

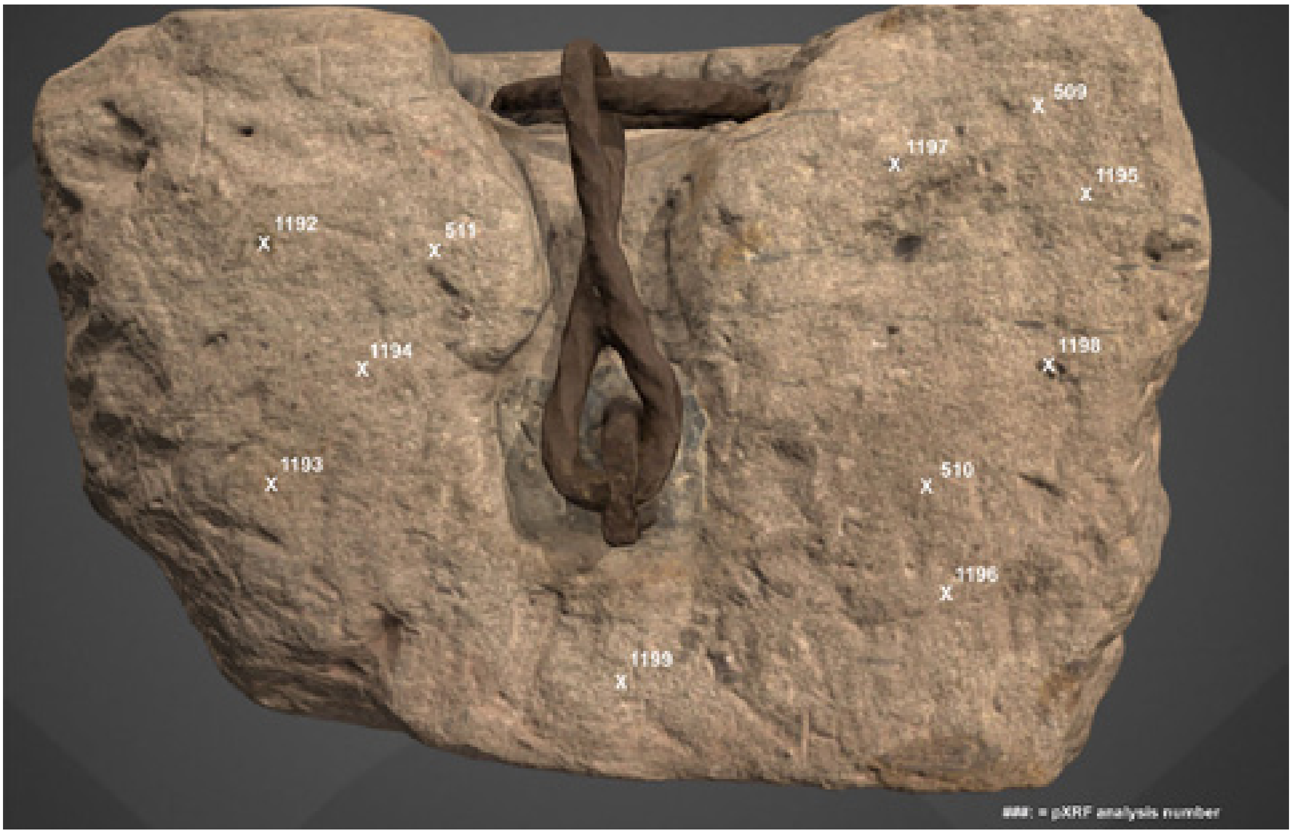

Fig 1e. Locations of pXRF analyses (8 mm diameter) on the dexter surface of the Stone of Destiny.

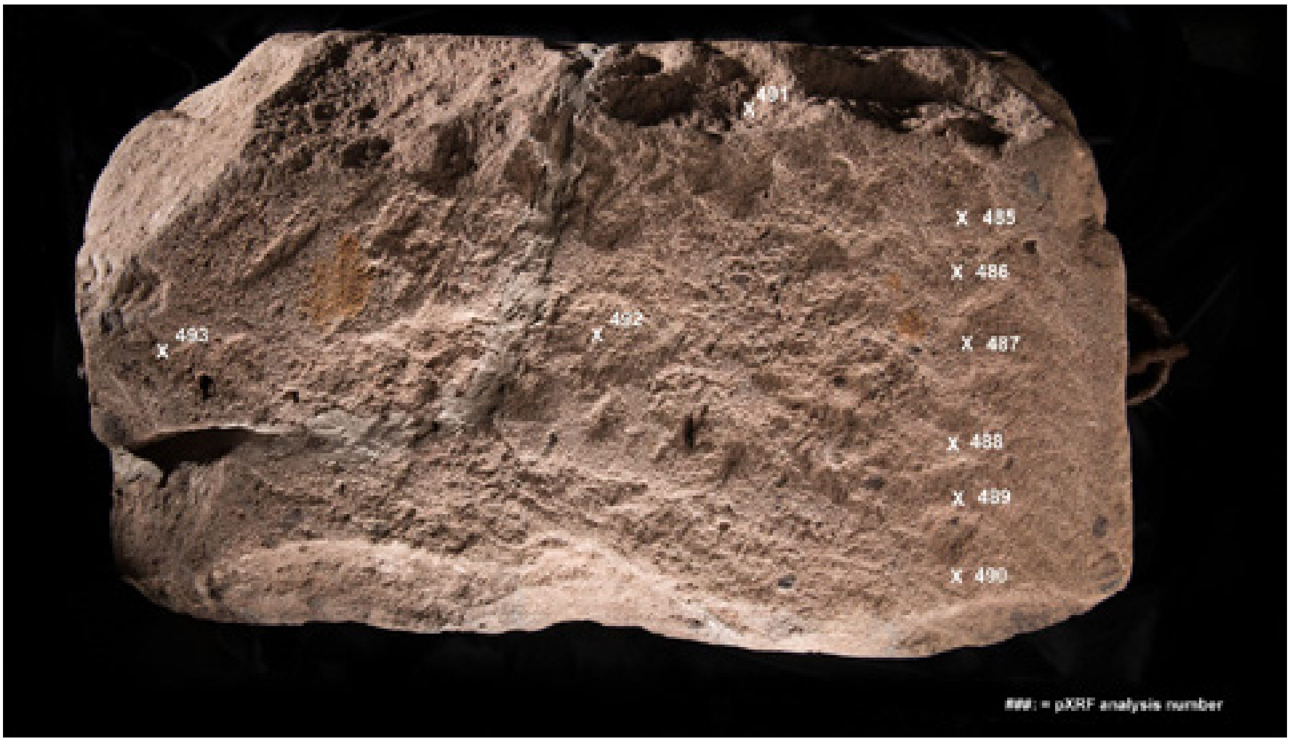

Fig 1f. Locations of pXRF analyses (8 mm diameter) on the Base surface of Stone of Destiny.

Results

Mean composition of Stone of Destiny sandstone

The mean chemical composition of each face, and of the Stone as a whole, were calculated from pXRF data as shown in Table 1. Results are consistent with the composition of a non-calcareous litharenite sandstone, variably contaminated by surface deposition of gypsum and other soiling.

Data were obtained from the intact Stone as analysis was required to be non-destructive. This introduces several potential sources of error into the results:

- The variable roughness of the surface introduces significant errors in pXRF results. This primarily affects lighter elements whose X-rays are preferentially attenuated in the air gap between the sample and the detector. Because X-rays from lighter elements are preferentially attenuated, normalisation of the data cannot wholly compensate for errors introduced as a result of surface roughness.
- The chemical elements detected by pXRF represent data mainly from the first few millimetres of the surface and will include components of weathering, alteration, soiling and staining. Heavier elements are detected at greater depth.
- Soluble components of the Stone may have been preferentially lost from the near surface.
- Elements which exist mainly as coatings on sandstone grain surfaces (such as iron) are likely to be over-represented in quantitative analysis.

Tables 1a-c. Results from normalised pXRF analysis of major elements at surfaces of the Stone of Destiny.*

Table 1a.

Mean amount *(standard deviation)*

Surface area	MgO (%)	Al_2O_3 (%)	SiO_2 (%)	P_2O_5 (%)	SO_3 (%)	Cl (%)	K_2O (%)	CaO (%)	TiO_2 (%)	MnO (%)	Fe_2O_3 (%)
Top	6.1 *(1.3)*	12.9 *(1.7)*	72.2 *(5.2)*	0.05 *(0.05)*	1.1 *(4.0)*	0.2 *(0.1)*	2.1 *(0.3)*	1.0 *(2.4)*	0.45 *(0.10)*	0.04 *(0.1)*	3.6 *(0.7)*
Base	4.8 *(1.5)*	7.9 *(3.2)*	72.4 *(3.2)*	< LOD *(NA)*	5.3 *(1.6)*	0.6 *(0.4)*	1.7 *(0.3)*	3.8 *(1.2)*	0.32 *(0.19)*	0.05 *(0.1)*	3.4 *(0.8)*
Front	4.8 *(1.4)*	10.1 *(0.6)*	75.7 *(1.6)*	0.00 *(0.00)*	1.9 *(0.7)*	0.1 *(0.1)*	2.0 *(0.3)*	1.2 *(0.4)*	0.40 *(0.06)*	0.05 *(0.1)*	3.7 *(0.5)*
Back	4.5 *(1.5)*	8.9 *(2.9)*	71.3 *(7.3)*	0.01 *(0.01)*	5.3 *(4.4)*	0.1 *(0.1)*	1.8 *(0.4)*	3.4 *(2.3)*	0.30 *(0.12)*	0.06 *(0.2)*	4.2 *(1.7)*
Dexter	4.4 *(1.6)*	8.3 *(1.9)*	68.9 *(6.7)*	0.01 *(0.01)*	6.8 *(5.0)*	0.3 *(0.1)*	1.8 *(0.2)*	4.3 *(3.0)*	0.40 *(0.15)*	0.05 *(0.1)*	4.5 *(1.0)*
Sinister	4.8 *(2.2)*	9.8 *(2.2)*	68.3 *(5.2)*	0.10 *(0.12)*	6.1 *(5.0)*	0.4 *(0.2)*	1.4 *(0.2)*	3.4 *(2.7)*	0.45 *(0.12)*	0.09 *(0.3)*	5.0 *(1.1)*
Mean	**5.3** ***(1.6)***	**10.6** ***(2.9)***	**71.7** ***(5.5)***	**0.05** ***(0.07)***	**3.4** ***(4.4)***	**0.2** ***(0.2)***	**1.9** ***(0.4)***	**2.3** ***(2.6)***	**0.40** ***(0.13)***	**0.05** ***(0.2)***	**3.9** ***(1.0)***

Limits of detection

MgO (%)	Al_2O_3 (%)	SiO_2 (%)	P_2O_5 (%)	SO_3 (%)	Cl (%)	K_2O (%)	CaO (%)	TiO_2 (%)	MnO (%)	Fe_2O_3 (%)
0.56	0.21	0.16	0.03	0.027	ND	0.010	0.013	0.01	0.00	0.012

Maximum

	MgO (%)	Al_2O_3 (%)	SiO_2 (%)	P_2O_5 (%)	SO_3 (%)	Cl (%)	K_2O (%)	CaO (%)	TiO_2 (%)	MnO (%)	Fe_2O_3 (%)
Top	9.0	15.6	78.0	0.17	22.0	0.4	2.6	13.7	0.69	0.05	5.2
Base	8.0	11.8	79.6	0.00	7.4	1.0	2.2	5.8	0.53	0.07	5.0
Front	6.8	10.7	78.0	0.00	2.9	0.3	2.4	1.8	0.49	0.06	4.5
Back	6.6	12.1	88.6	0.02	14.2	0.2	2.2	8.5	0.42	0.11	7.7
Dexter	7.3	10.5	74.9	0.02	18.6	0.5	2.0	11.4	0.71	0.08	5.7
Sinister	9.5	12.9	74.7	0.33	16.9	0.6	1.6	9.2	0.60	0.13	6.8

Minimum

	MgO (%)	Al_2O_3 (%)	SiO_2 (%)	P_2O_5 (%)	SO_3 (%)	Cl (%)	K_2O (%)	CaO (%)	TiO_2 (%)	MnO (%)	Fe_2O_3 (%)
Top	2.5	6.7	48.6	0.00	0.1	0.1	1.2	0.4	0.26	0.03	2.4
Base	2.8	2.2	69.1	0.00	3.0	0.2	1.3	1.9	0.05	0.02	2.4
Front	3.0	9.3	73.0	0.00	0.8	0.0	1.6	0.7	0.34	0.04	3.0
Back	2.5	3.1	61.6	0.00	0.5	0.1	1.0	1.5	0.03	0.04	1.6
Dexter	2.0	5.8	55.7	0.00	2.1	0.1	1.4	1.5	0.22	0.03	3.3
Sinister	2.4	6.7	58.7	0.00	2.7	0.2	0.9	1.7	0.28	0.06	3.6

**Sample locations in Figure 1. The composition of each surface is the mean of the following numbers of analyses: Top 30, Front 8, Back 10, Sinister 7, Dexter 8, Base 9 sample positions. Analyses of inclusions and obvious surface deposits have been excluded (14 samples). < LOD = below limit of detection. ND = not determined. NA = not applicable.*

Table 1b.

Mean amount *(standard deviation)*

Surface area	V (ppm)	Cr (ppm)	Ni (ppm)	Cu (ppm)	Zn (ppm)	Ga (ppm)	As (ppm)	Rb (ppm)	Sr (ppm)	Y (ppm)	Zr (ppm)
Top	140 *(26)*	117 *(95)*	31 *(6)*	58 *(15)*	236 *(140)*	10 *(3)*	11 *(3)*	60 *(10)*	136 *(17)*	2 *(2)*	156 *(43)*
Base	214 *(92)*	243 *(228)*	37 *(13)*	57 *(24)*	63 *(22)*	15 *(6)*	< LOD *(NA)*	80 *(27)*	180 *(28)*	17 *(31)*	234 *(97)*
Front	160 *(16)*	93 *(38)*	35 *(13)*	153 *(159)*	95 *(64)*	15 *(6)*	29 *(22)*	73 *(9)*	179 *(15)*	4 *(5)*	206 *(64)*
Back	232 *(178)*	117 *(85)*	42 *(22)*	52 *(30)*	94 *(43)*	14 *(7)*	93 *(159)*	82 *(33)*	161 *(32)*	13 *(23)*	237 *(80)*
Dexter	180 *(42)*	115 *(52)*	43 *10()*	51 *(10)*	73 *(15)*	16 *(5)*	17 *(2)*	83 *(24)*	195 *(34)*	5 *(4)*	227 *(78)*
Sinister	192 *(11)*	141 *(132)*	70 *(19)*	77 *(35)*	233 *(78)*	17 *(13)*	169 *(219)*	57 *(10)*	174 *(25)*	2 *(3)*	210 *(23)*
Mean	**164** ***(74)***	**127** ***(108)***	**39** ***(17)***	**69** ***(62)***	**160** ***(124)***	**13** ***(6)***	**76** ***(137)***	**69** ***(21)***	**160** ***(32)***	**6** ***(15)***	**196** ***(70)***

Limits of detection

V (ppm)	Cr (ppm)	Ni (ppm)	Cu (ppm)	Zn (ppm)	Ga (ppm)	As (ppm)	Rb (ppm)	Sr (ppm)	Y (ppm)	Zr (ppm)
64	29	8	7	6	3	7	3	4	3	6

Maximum

	V (ppm)	Cr (ppm)	Ni (ppm)	Cu (ppm)	Zn (ppm)	Ga (ppm)	As (ppm)	Rb (ppm)	Sr (ppm)	Y (ppm)	Zr (ppm)
Top	199	546	43	95	553	16	13	88	188	9	276
Base	279	581	62	96	97	27	0	123	227	77	434
Front	178	130	54	535	246	20	45	85	197	13	330
Back	547	315	94	135	206	32	449	165	231	77	428
Dexter	224	199	57	61	100	23	18	124	240	10	396
Sinister	200	434	99	133	332	35	422	73	220	6	238

Minimum

	V (ppm)	Cr (ppm)	Ni (ppm)	Cu (ppm)	Zn (ppm)	Ga (ppm)	As (ppm)	Rb (ppm)	Sr (ppm)	Y (ppm)	Zr (ppm)
Top	97	42	20	34	88	4	8	48	108	0	101
Base	149	76	21	31	38	9	0	42	143	0	138
Front	148	40	21	71	55	8	14	60	153	0	131
Back	133	56	18	29	49	5	10	40	99	0	168
Dexter	141	45	30	35	53	9	16	63	149	0	142
Sinister	184	49	47	37	119	7	34	43	146	0	176

Table 1c.

Mean amount *(standard deviation)*

Surface area	Nb (ppm)	Ba (ppm)	Pb (ppm)	Ce (ppm)	Pd (ppm)	Ag (ppm)	Cd (ppm)	Sn (ppm)	Sb (ppm)	Te (ppm)	Hg (ppm)
Top	6 *(3)*	660 *(151)*	319 *(927)*	0 *(0)*	5 *(10)*	0 *(0)*	0 *(0)*	< LOD *(NA)*	35 *(NA)*	1 *(NA)*	< LOD *(NA)*
Base	9 *(3)*	1164 *(453)*	51 *(29)*	< LOD *(NA)*	19 *(21)*	0 *(0)*	< LOD *(NA)*	< LOD *(NA)*	< LOD *(NA)*	< LOD *(NA)*	< LOD *(NA)*
Front	7 *(1)*	901 *(139)*	26 *(4)*	< LOD *(NA)*	8 *(12)*	0 *(0)*	< LOD *(NA)*	< LOD *(NA)*	< LOD *(NA)*	< LOD *(NA)*	101 *(NA)*
Back	11 *(9)*	969 *(479)*	53 *(73)*	115 *(NA)*	11 *(20)*	0 *(NA)*	< LOD *(NA)*	< LOD *(NA)*	43 *(NA)*	2 *(0)*	< LOD *(NA)*
Dexter	7 *(1)*	1133 *(529)*	475 *(782)*	313 *(192)*	0 *()*	< LOD *(NA)*	< LOD *(NA)*	< LOD *(NA)*	< LOD *(NA)*	2 *(0)*	< LOD *(NA)*
Sinister	7 *(0)*	771 *(209)*	586 *(588)*	< LOD *(NA)*	52 *(NA)*	0 *(0)*	13 *(NA)*	< LOD *(NA)*	39 *(NA)*	1 *(0)*	< LOD *(NA)*
Mean	**7** ***(4)***	**856** ***(367)***	**259** ***(690)***	**62** ***(135)***	**12** ***(18)***	**0** ***(0)***	**6** ***(9)***	**< LOD** ***(NA)***	**39** ***(4)***	**1** ***(0)***	**101** ***(NA)***

Limits of detection

Nb (ppm)	Ba (ppm)	Pb (ppm)	Ce (ppm)	Pd (ppm)	Ag (ppm)	Cd (ppm)	Sn (ppm)	Sb (ppm)	Te (ppm)	Hg (ppm)
3	57	8	ND	ND	ND	ND	ND	22	ND	ND

Maximum

	Nb (ppm)	Ba (ppm)	Pb (ppm)	Ce (ppm)	Pd (ppm)	Ag (ppm)	Cd (ppm)	Sn (ppm)	Sb (ppm)	Te (ppm)	Hg (ppm)
Top	17	1250	5141	0	23	0	0	0	35	1	0
Base	14	1900	105	0	51	0	0	0	0	0	0
Front	9	1094	31	0	17	0	0	0	0	0	101
Back	28	2293	218	115	34	0	0	0	43	2	0
Dexter	8	2059	2334	449	0	0	0	0	0	2	0
Sinister	8	1224	1792	0	52	0	13	0	39	1	0

Minimum

	Nb (ppm)	Ba (ppm)	Pb (ppm)	Ce (ppm)	Pd (ppm)	Ag (ppm)	Cd (ppm)	Sn (ppm)	Sb (ppm)	Te (ppm)	Hg (ppm)
Top	3	474	29	0	0	0	0	0	35	1	0
Base	6	694	17	0	0	0	0	0	0	0	0
Front	5	753	19	0	0	0	0	0	0	0	101
Back	7	657	12	115	0	0	0	0	43	1	0
Dexter	6	703	66	177	0	0	0	0	0	1	0
Sinister	7	627	72	0	52	0	13	0	39	1	0

Based on digital portable microscope results, observations are consistent with previous thin section analysis from Fortey et al. (1998).

The Stone is moderately sorted and fine to predominantly medium grained, displaying a mean grain size of ~0.2–0.35 mm, with occasional larger **grains** of ~0.4-0.5 mm and pebbles which measure >1 cm in length. Individual grains appear elongate to spherical and angular to sub-rounded in shape. Grains are surrounded by a light-coloured **intergranular material** (cementing minerals or clays) which is variable in its distribution throughout the observed areas of the Stone.

Microscope observations are consistent with a **mineralogically immature** sandstone and show a mixture of:

- clear, unstained and glassy textured grains, through to iron-stained and rose-tinted quartz grains;
- elongate flakes of **mica** (both dark and light variants; probably biotite and muscovite, respectively);
- mixed indiscernible lithic fragments, iron nodules and other iron-stained grains, larger grains or pebbles (cm in scale) including quartz and mudstone.

Detailed observations in Figure 2 of one large quartz pebble (location 1155 in Fig 1a) highlighted numerous narrow scratch marks, measuring between 0.02–0.006 mm in thickness. These scratch marks appear to be post-depositional and are unlikely to be geological in origin. They could relate to in-service abrasion of the Stone post-extraction from the quarry, or to abrasion from tools used to shape and hone the Stone.

Fig 2. Microscope image of scratch marks on a large pebble on the top surface of the Stone of Destiny.

Variations in composition of surfaces

Sulphate and the question of whether the sandstone is calcareous

Several of the locations analysed were notably high in sulphate (SO_3) – up to ~22%. Sulphate concentrations were commonly >2%, but with a high standard deviation (Table 1a). There was a strong correlation with **calcium oxide** (CaO) (Fig 3) which implies that both CaO and SO_3 concentrations were mainly attributable to the presence of gypsum ($CaSO_4.2H_2O$) contamination of surfaces.

The trendline in Figure 3 indicates that at 0% SO_3, the CaO content of the sandstone would be 0.3%. Allowing for some variation in the SO_3 content of unsoiled sandstone, CaO levels in the absence of gypsum are likely to be <1%, implying that the Stone of Destiny is not calcareous (or that any pre-existing calcareous minerals or cements near the surface have dissolved).[3]

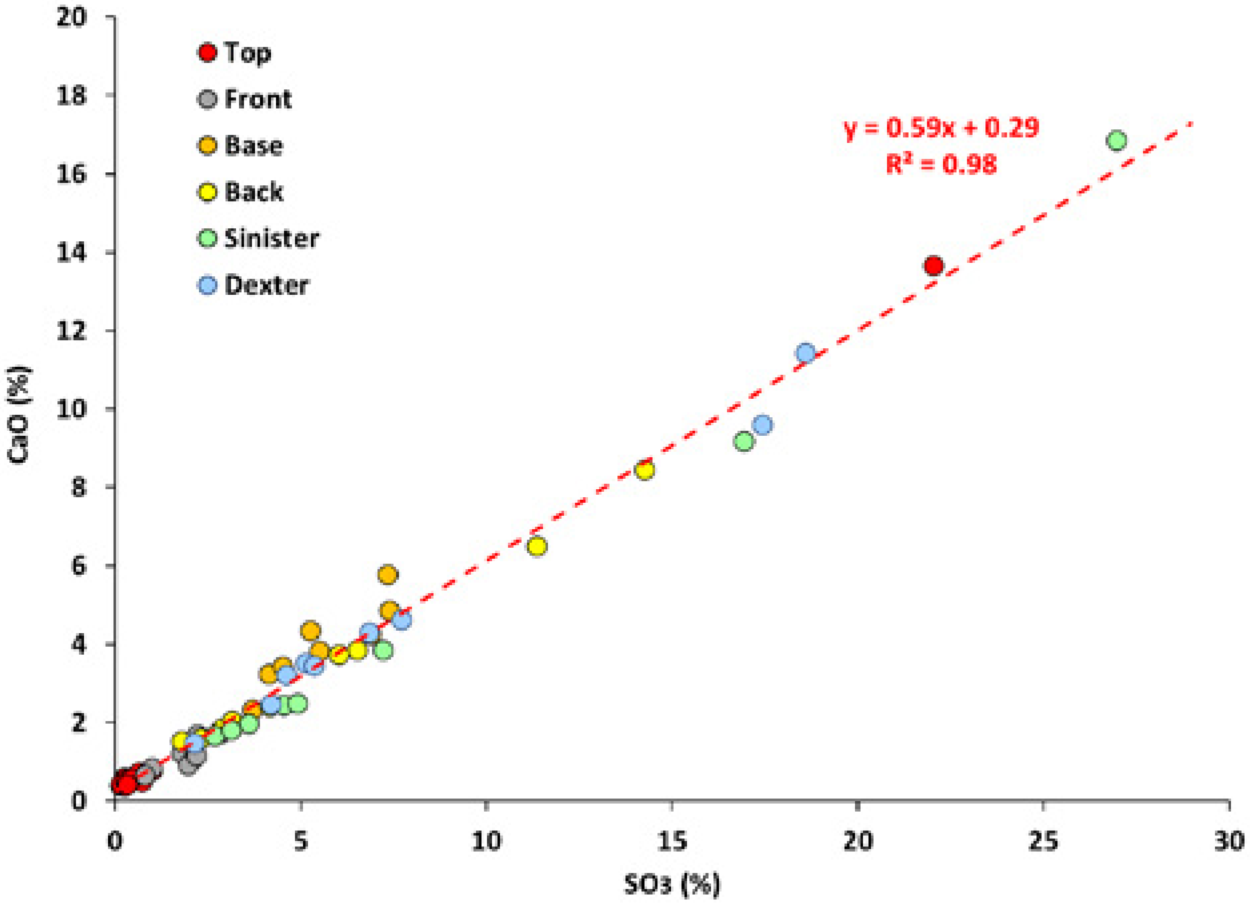

Fig 3. Correlation between CaO and SO_3 concentrations (normalised pXRF data) at sample locations on various surfaces of the Stone of Destiny.

The presence of gypsum is an indication of surface contamination. Gypsum can be deposited from sulphates in historic air pollution, but gypsum from air pollution is normally black due to incorporation of soot particles. The gypsum found here (data from digital portable microscope, Figure 4a) is white and pore filling. It appears to contain small, white, unmixed lumps of gypsum and an inherent **aggregate** component (inferred from the relative smaller grain size of minerals within the region of gypsum deposition compared to the Stone in Fig 4a). The presence of an aggregate component would be indicative of a composite gypsum material having been applied to the Stone as opposed to an environmental contamination source. Perhaps gypsum residues are a consequence of a mould being taken from the Stone at some time in the past? At present, no such event is known to have occurred.

The highest concentration of gypsum (~36%) was detected on the top surface in the recess of one of the lifting rings (Figs 3 and 4a). Smoother areas of the top surface had relatively low levels of gypsum (Fig 4b). Variable amounts were observed on the other surfaces examined (Fig 5). Overall, samples analysed on the top and front surfaces had lower sulphate concentrations and samples from the base, back, sinister and dexter surfaces had higher sulphate concentrations. The cause of these differences is not known.

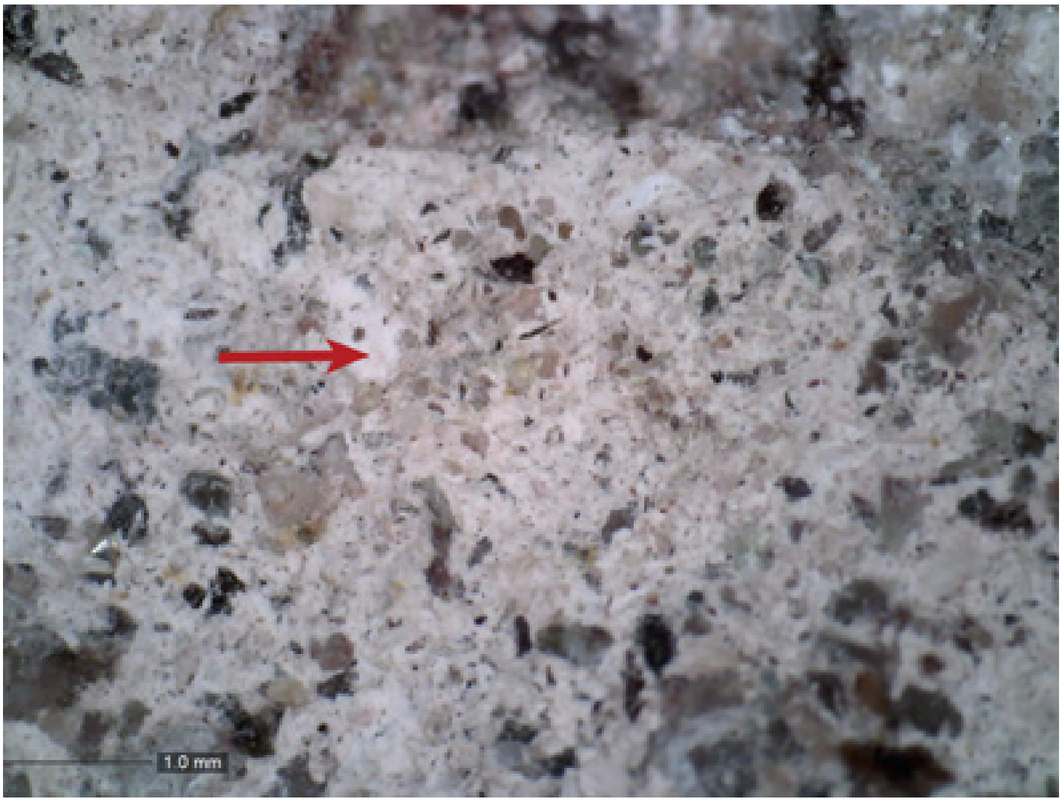

Fig 4a. Sample area 500. Magnified image of an area of white deposited material on the top surface. Lump of unmixed gypsum highlighted by red arrow.

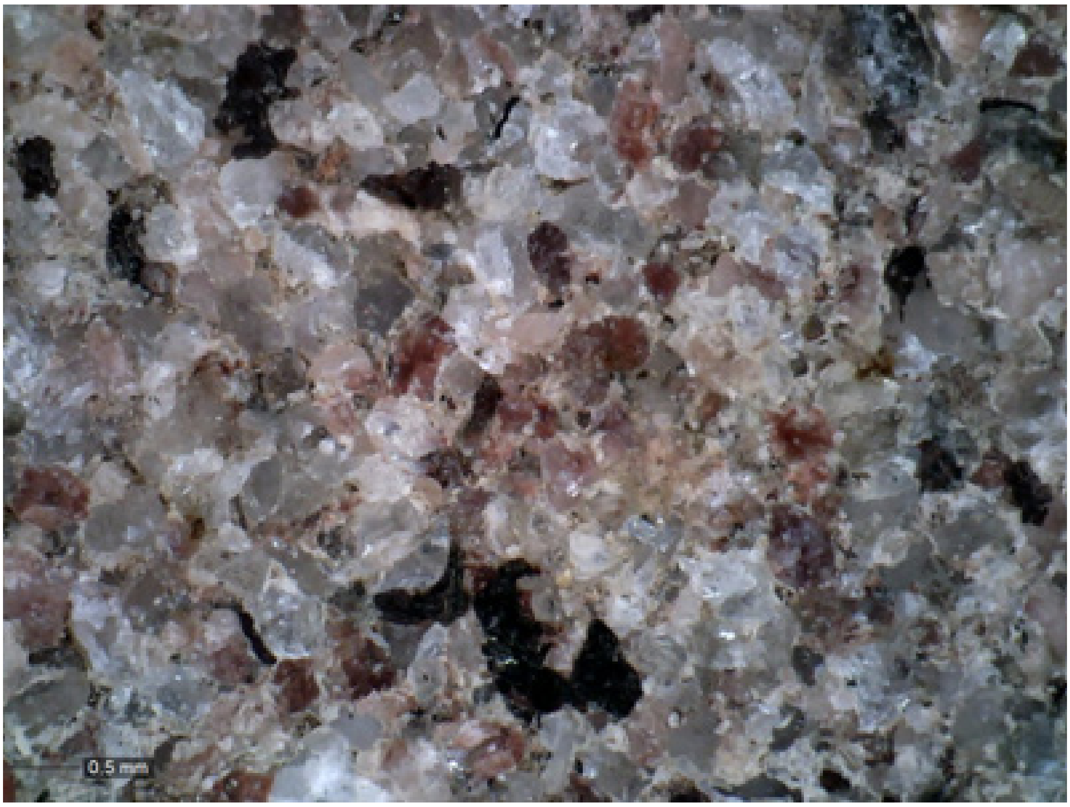

Fig 4b. Sample area 503. Smooth area of stone on the top surface. Note the relatively open mineral texture and absence of intergranular geological material.

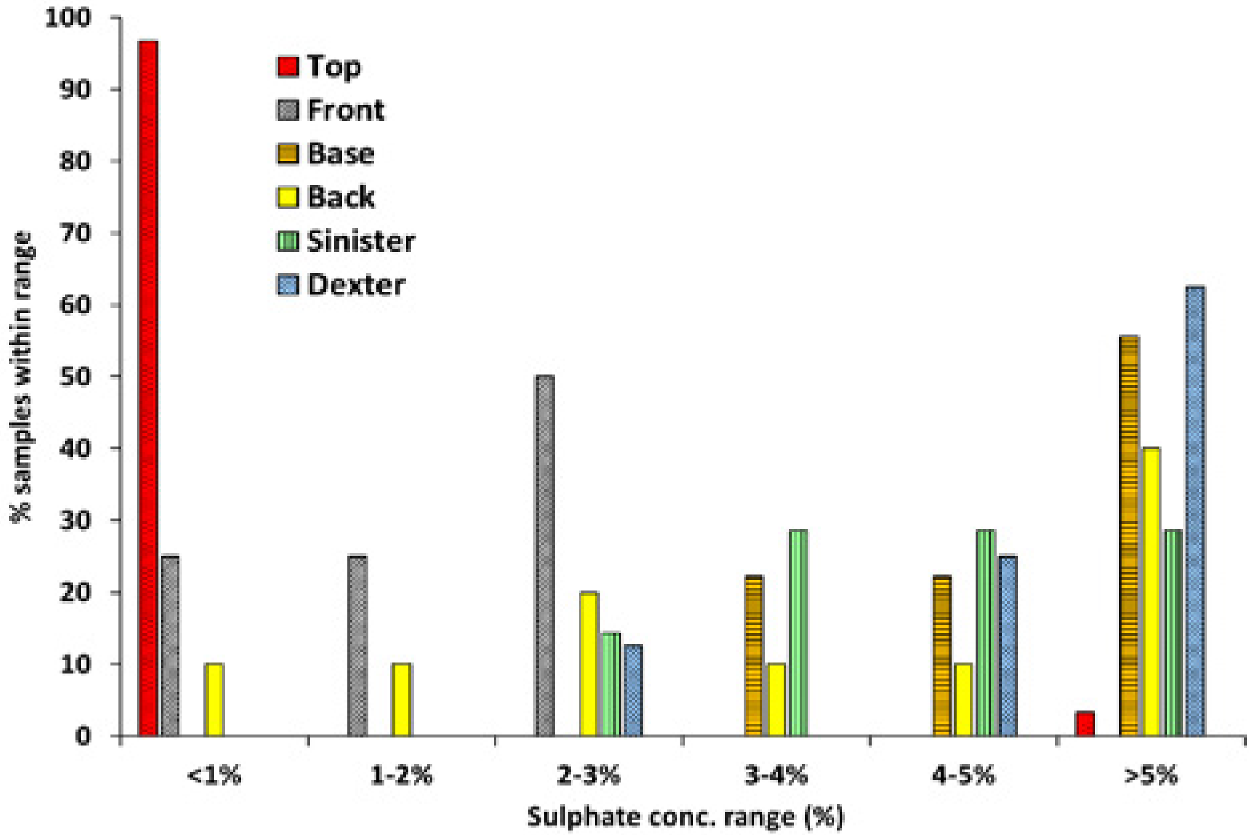

Fig 5. Percentages of sample sulphate concentrations within specific ranges.

Zinc concentrations

There is a dark, roughly 'heart' shaped patch on the top surface of the Stone of Destiny (see upper centre Fig 1a, sample numbers 501, 502, 1158, 1159, 1160, 1161 & 1180). pXRF analysis indicates that this area has a significantly higher concentration of zinc compared to adjacent areas (Fig 7).[4]

The source of the zinc is not known. It is unlikely that the zinc concentration is an original component of the sandstone. The date of the first observation of the stain is not known. It is possibly derived from a zinc-rich material or object having been in contact with the top surface. There are no obvious correlations with any other chemical elements in the pXRF analyses of the Stone.

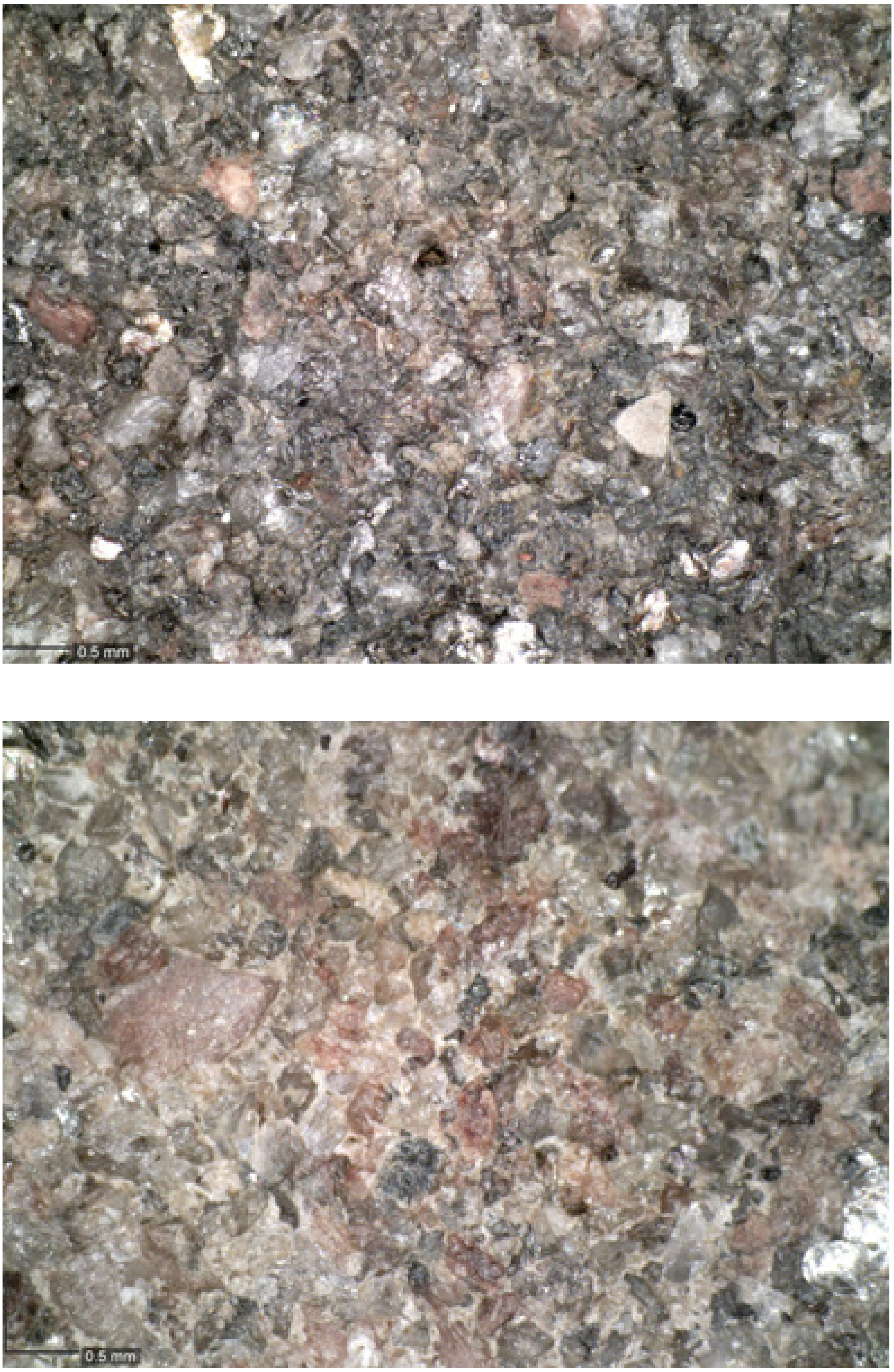

Fig 6. Difference in appearance between dark 'heart' shaped patch and an area of unstained stone on the top surface of the Stone of Destiny. Above: Sample area 1160 – dark surface staining on grains. Below: Sample area 1169 – clean open mineral texture on an adjacent area of non-stained stone.

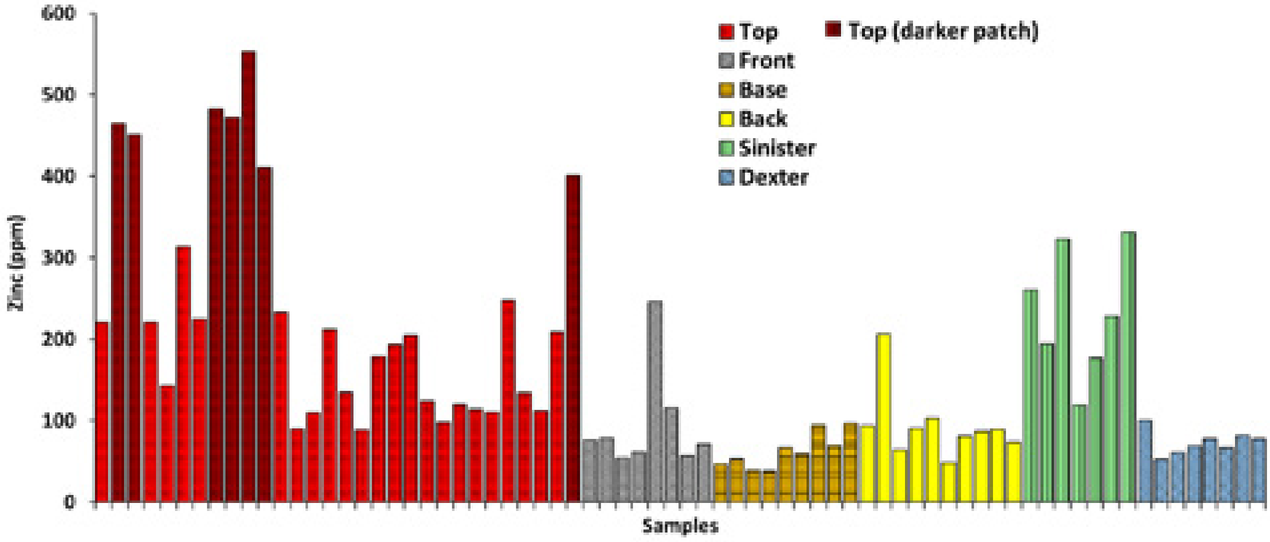

Fig 7a. Zinc concentrations on sampled areas of surfaces of the Stone of Destiny. Zinc concentrations on the darker stained area on the top surface are indicated in dark red.

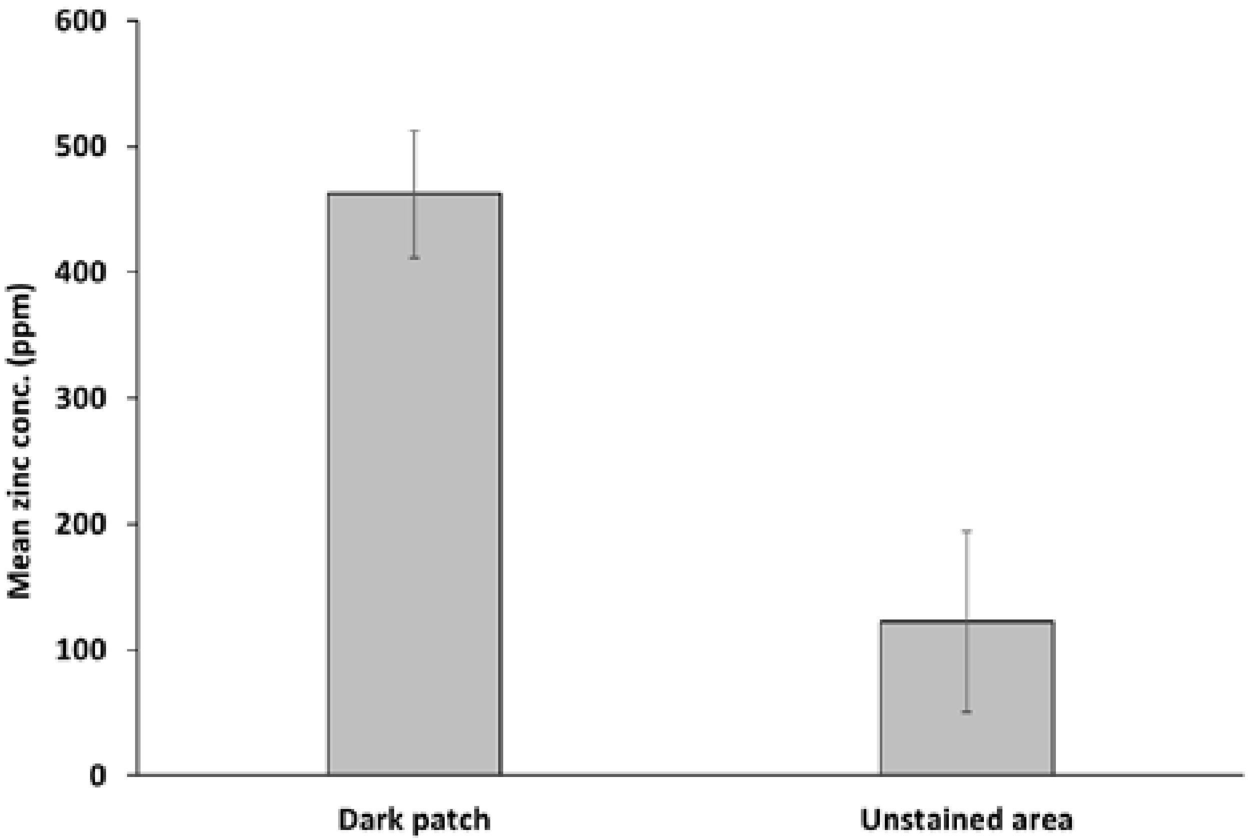

Fig 7b. Mean zinc concentrations on dark stained (7 analysis locations) and unstained (23 analysis locations) areas on the top surface of the Stone of Destiny.

Arsenic concentrations

Arsenic was detected by pXRF analysis at below the level of detection (< LOD) or in low concentrations at most analysis locations (Fig 8). Higher concentrations of arsenic occurred on a few locations on the back and sinister surfaces of the Stone of Destiny.

Arsenic in higher concentrations is presumed to have come from pigments in paint, known to be present on the Coronation Chair. These could have been transferred to the Stone of Destiny by contact with painted surfaces.

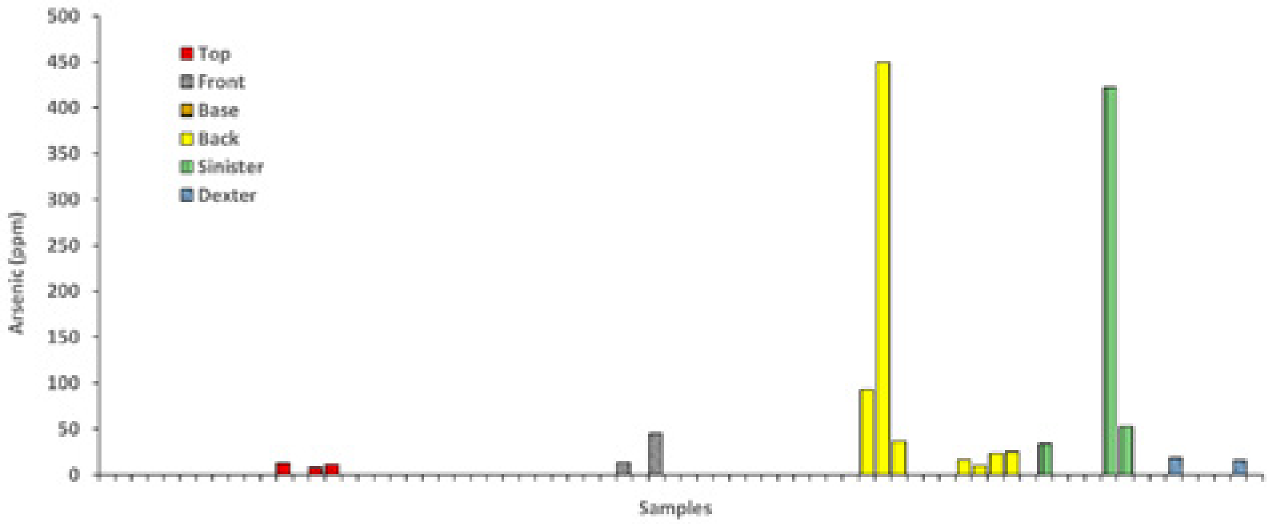

Fig 8. Arsenic concentrations on sampled areas of surfaces of the Stone of Destiny.

Phosphate concentrations

Phosphate (P_2O_5) was below the level of detection (< LOD) for most sample locations. Higher concentrations were found mainly on the top and sinister surfaces (Fig 9). The cause of these phosphate concentrations is not known.

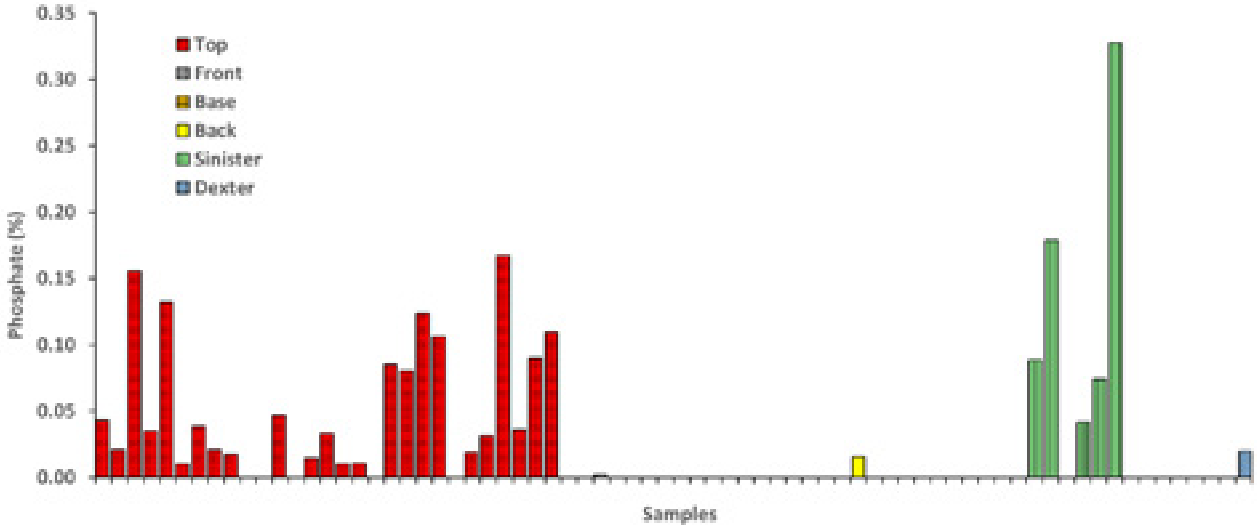

Fig 9. Phosphate (P_2O_5) concentrations on sampled areas of surfaces of the Stone of Destiny.

Chromium concentrations

Several analysis locations from surfaces of the Stone of Destiny had elevated levels of chromium (Cr) (Fig 10). It is suggested that locally elevated concentrations of chromium are related to the use of more modern tools (potentially a component of either steel or paint) for moving the Stone of Destiny in and out of the Coronation Chair in the 20th century.

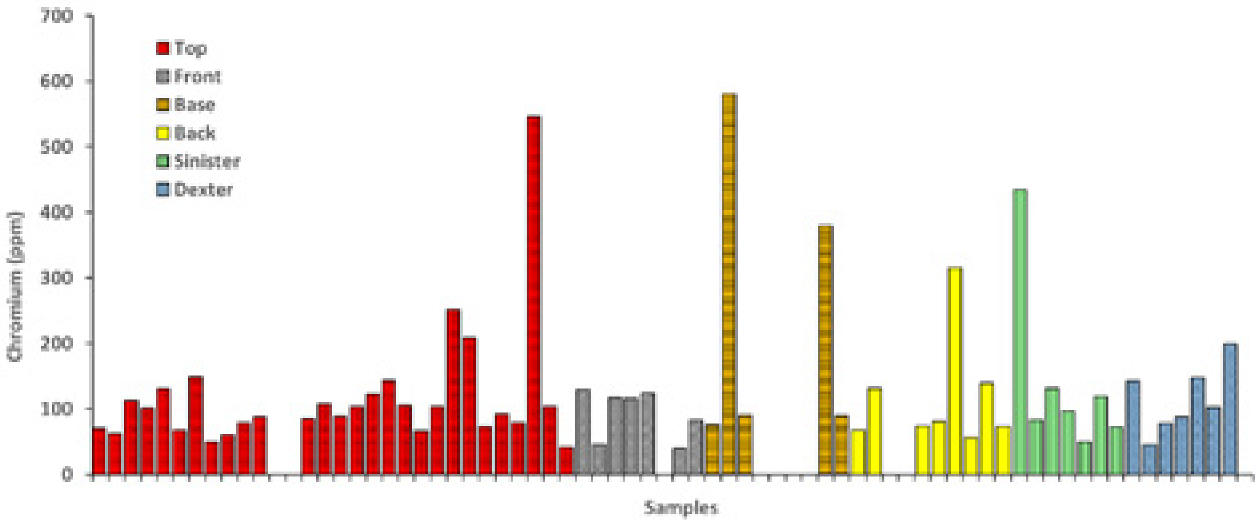

Fig 10. Chromium (Cr) concentrations on sampled areas of surfaces of the Stone of Destiny.

Roman numeral incisions

Three previously unrecorded incisions were identified on a small recess at the base of the back surface during condition survey checks in January 2023 (Fig 1c). The incisions comprise three 'X' marks, which have the appearance of Roman numerals. The individual lines within each 'X' incision measure ~1 mm in width (Fig 11) and must therefore correspond to the use of a very fine chisel or cutting instrument.

Deposited material

Five locations (near pXRF analysis positions 485, 487, 488, 490 & 493. See Fig 1f) on the base of the Stone of Destiny had small patches of an unknown red material (Fig 12). They appear visually distinct from the geological composition of the Stone and display a different red hue to iron-bearing minerals observed elsewhere in the Stone. These red deposits were varied in size, shape and distribution. There were no obvious anomalies in the pXRF data corresponding to their presence on the Stone. The source of this red material is unknown.

Comparatively large patches of blue material were present on the dexter face and base of the Stone (Fig 13). The patches of blue are different in texture to the red material and may represent paint transfer from tools previously used to move/transport the Stone in the 20th century.

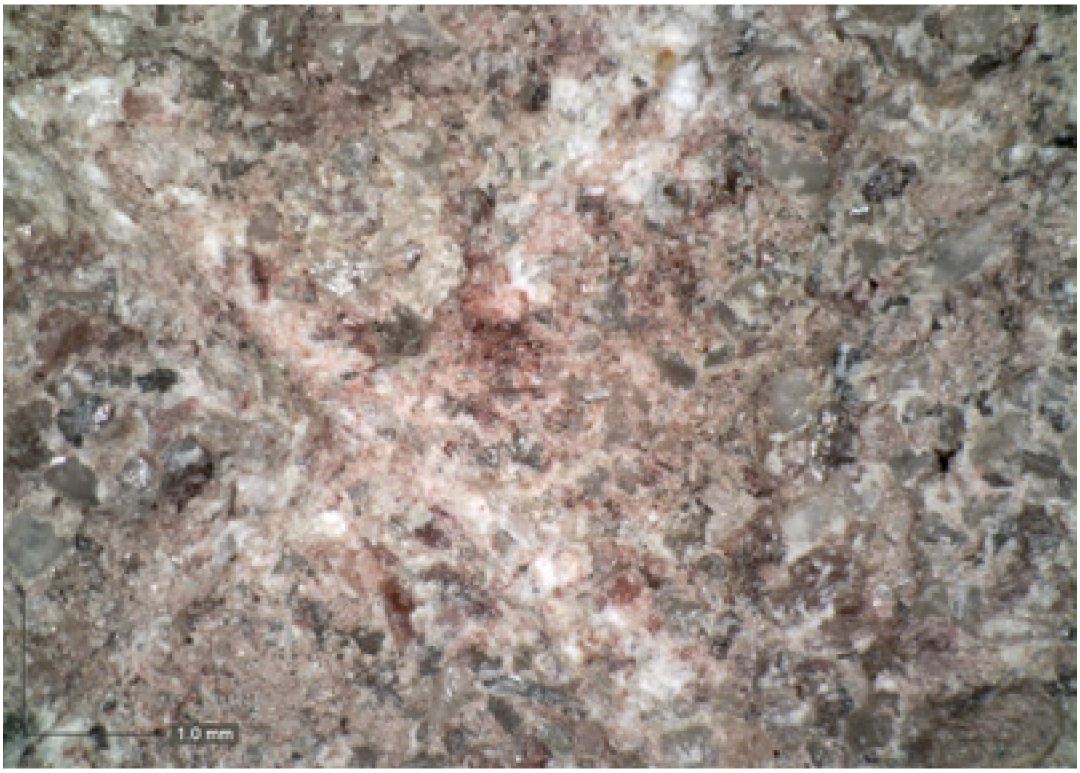

Fig 11. Microscope image of the middle of the three 'x' incisions. Location shown in Fig 1c.

Fig 12. Sample analysis area 487 showing an accumulation of deposited red material (centre right of image).

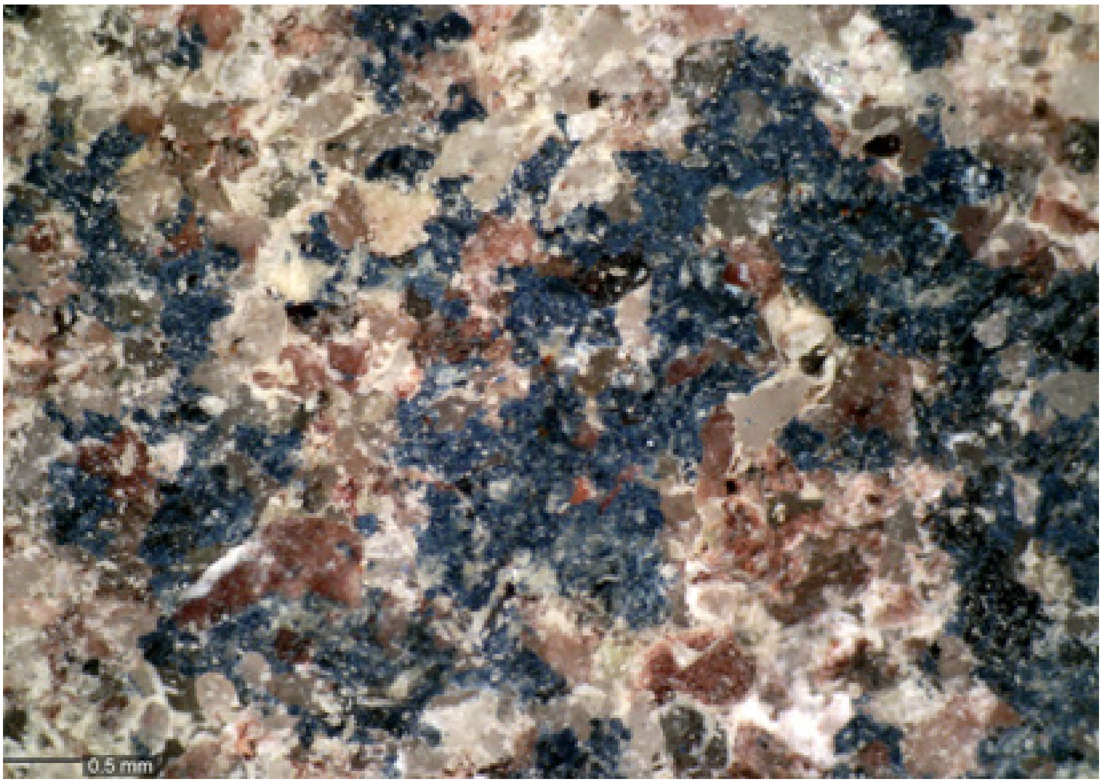

Fig 13. Blue deposited/transferred material on the base of the Stone of Destiny.

Colour analysis

Figure 14 shows the results of colour analysis of the Stone of Destiny. The results show only results for the Stone itself; inclusions and obvious surface deposits have been excluded. There is some variation between faces of the Stone. The main trend visible in coloration is for dark stained areas on the top surface (see 'Zinc concentrations' above), which are darker (L*), less red (a*) and less yellow (b*).

Zinc concentrations were found to correlate with the coloration of the Stone of Destiny (Fig 15). Higher zinc concentrations resulted in darker, less red and less yellow surfaces.

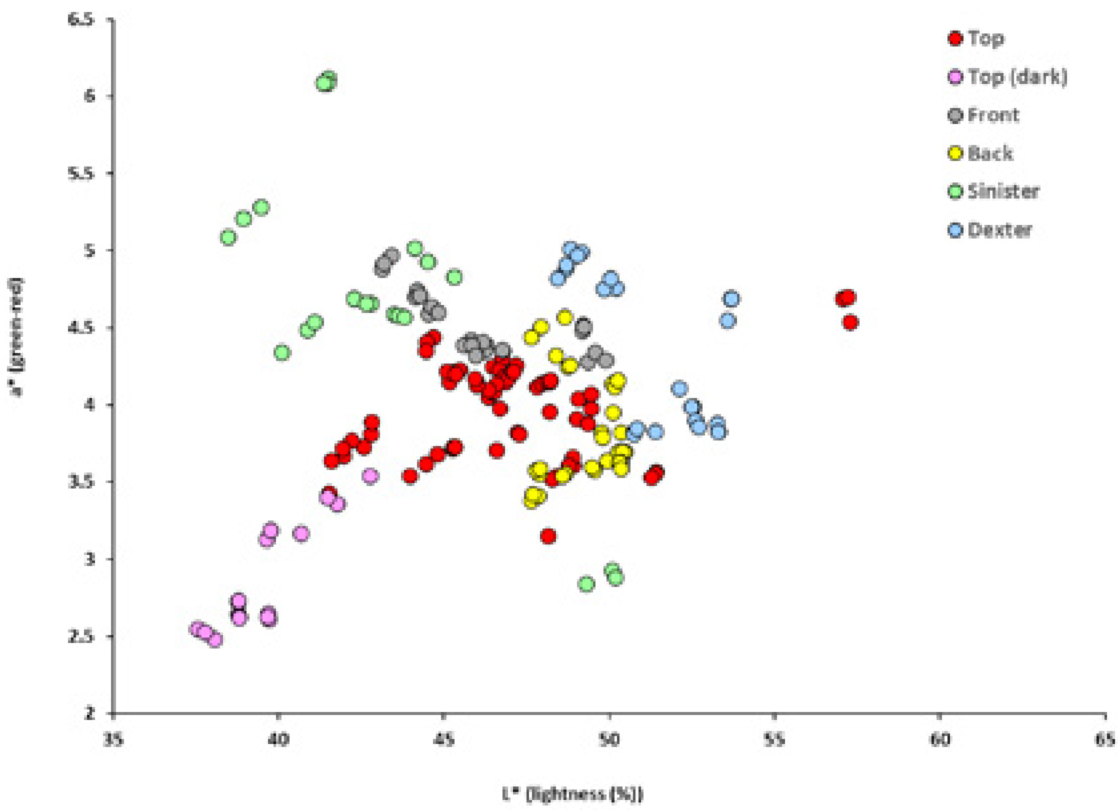

Fig 14a. Colour analysis of stone (excluding inclusions and surface deposits). L (lightness) vs. a* (green-red coloration).*

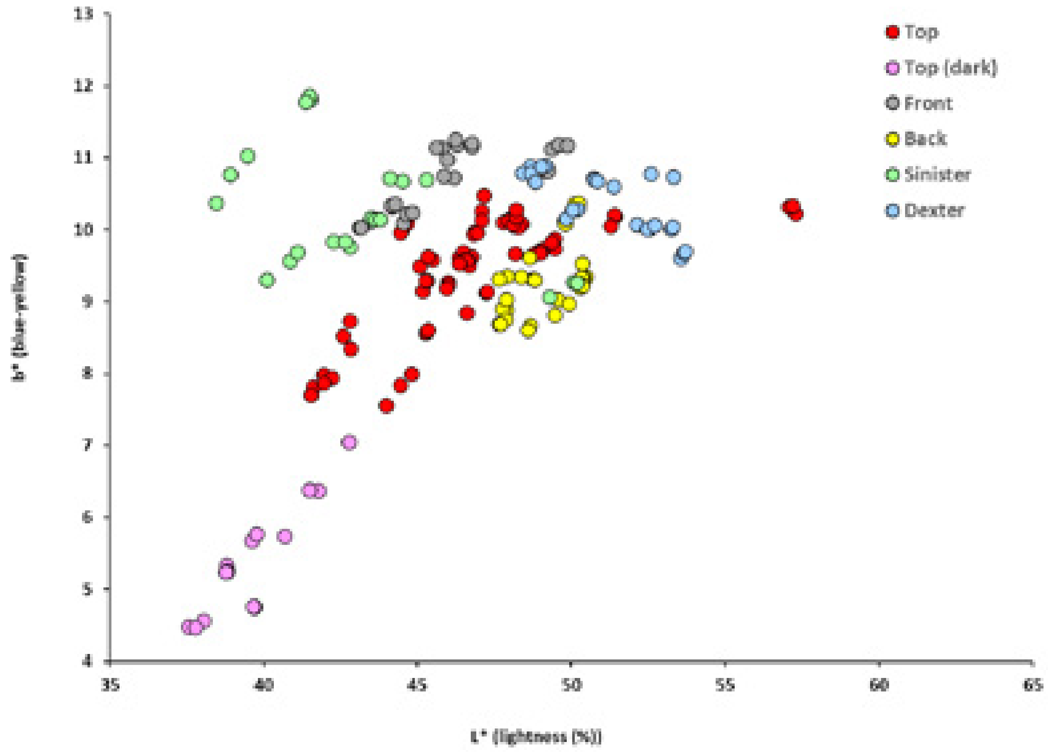

Fig 14b. Colour analysis of stone (excluding inclusions and surface deposits). L (lightness) vs. b* (blue-yellow coloration).*

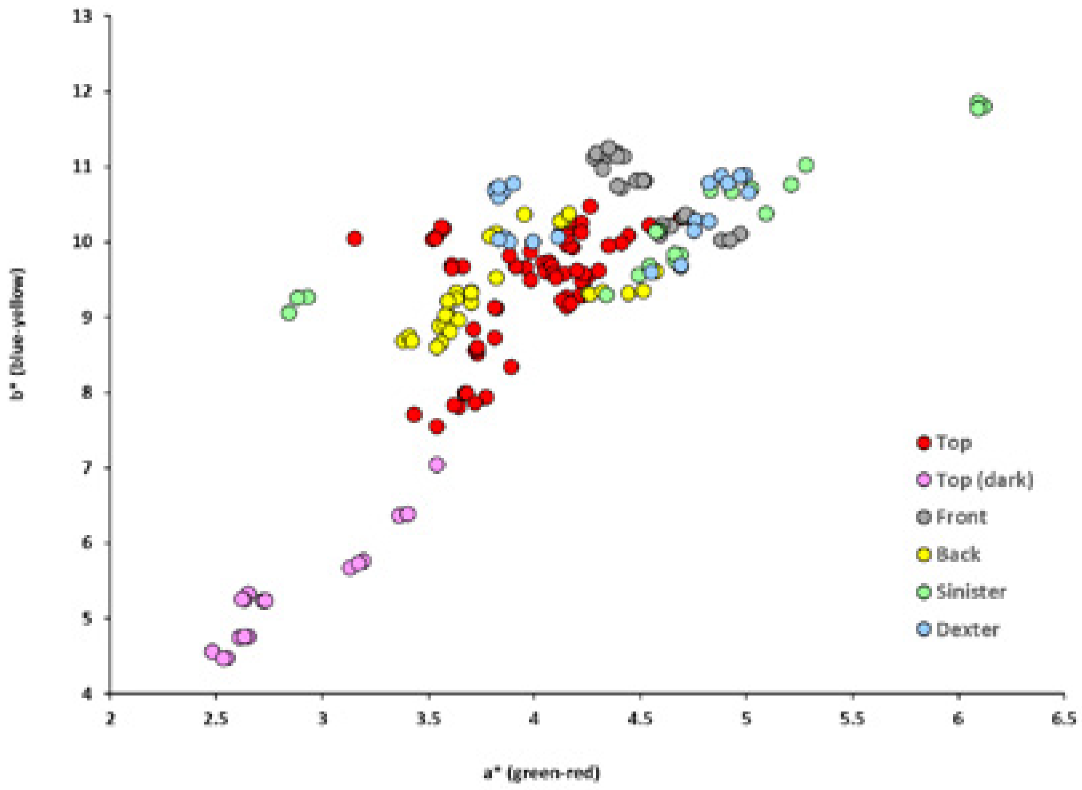

Fig 14c. Colour analysis of stone (excluding inclusions and surface deposits). a (green-red coloration) vs. b* (blue-yellow coloration).*

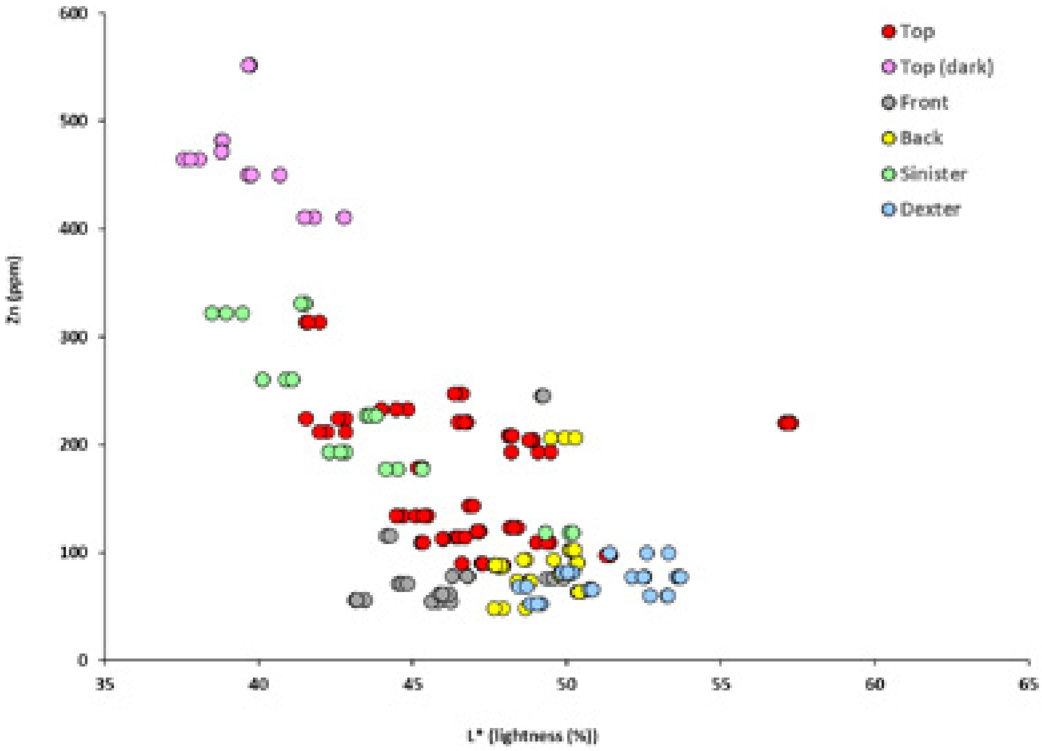

Fig 15a. Correlation between zinc concentration and lightness in coloration (L) of stone (excluding inclusions and surface deposits).*

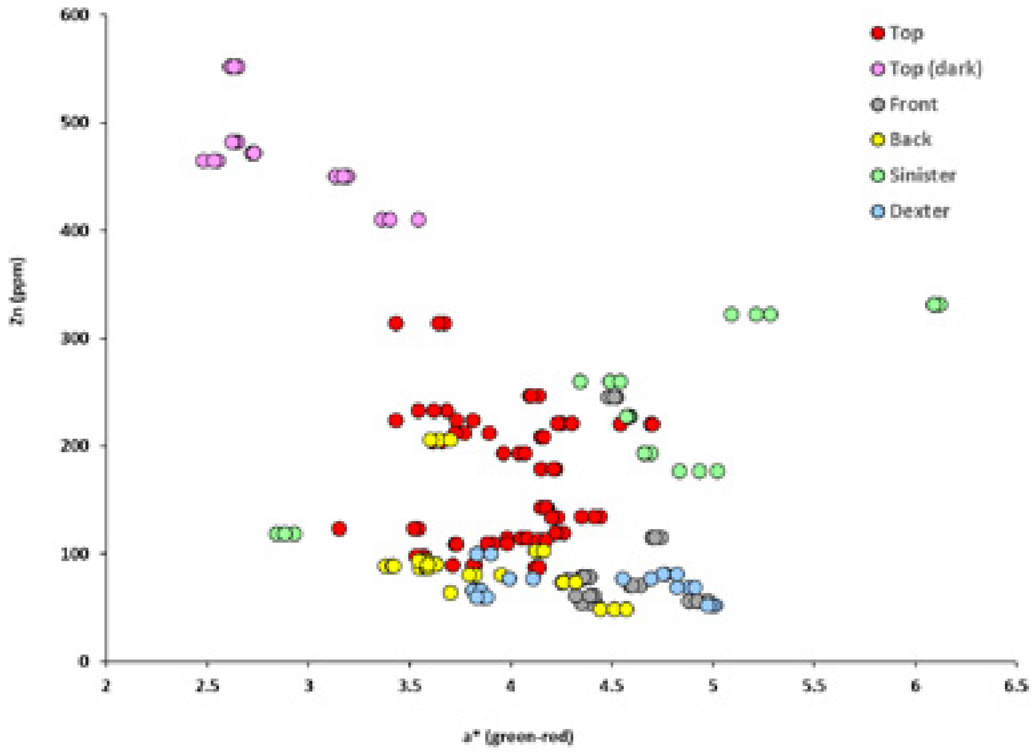

Fig 15b. Correlation between zinc concentration and green-red coloration (a) of stone (excluding inclusions and surface deposits).*

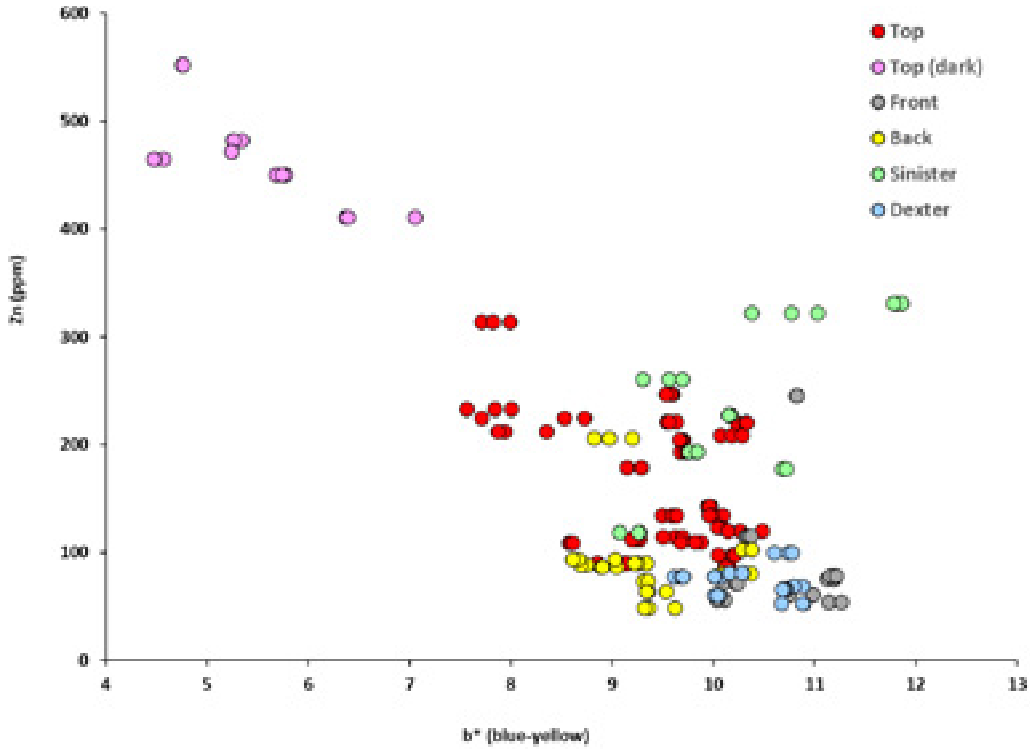

Fig 15c. Correlation between zinc concentration and blue-yellow coloration (b) of stone (excluding inclusions and surface deposits).*

Conclusions

Results of the investigation are summarised as follows:

- Based on portable microscope analysis, the Stone is moderately sorted, fine to medium grained and mineralogically immature. Observations are consistent with thin section analysis from Fortey et al (1998)[1], the sandstone type being described as litharenite.
- Based on pXRF results, the mean composition of the Stone of Destiny sandstone is consistent with the composition of a non-calcareous sandstone.
- Several sample locations were notably high in sulphate (SO_3)–up to ~22%. Sulphate concentrations on sampled areas were commonly >2%. There was a strong correlation on all analysed locations between sulphate and calcium oxide (CaO) concentrations, implying that both CaO and SO_3 were mainly attributable to the presence of gypsum ($CaSO_4.2H_2O$).
- Gypsum is likely to be indicative of surface contamination. Possible sources are historic air pollution or residue from a mould having been taken from the Stone at some time in the past. No such event is currently known to have occurred.
- The top and front surfaces generally had lower levels of gypsum contamination. The base, back, sinister and dexter surfaces generally had higher levels of gypsum contamination.
- The highest concentration of gypsum (~36%) was detected on the top surface in the

recess of one of the lifting rings. Smoother areas of the top surface had low levels of gypsum.

- Calcium oxide concentrations in the Stone of Destiny in the absence of gypsum are likely to be <1%, implying that the Stone of Destiny is not calcareous (or that any pre-existing calcareous minerals or cements have been lost by **dissolution**).
- There is a dark ‘heart’-shaped patch on the top surface of the Stone of Destiny. pXRF analysis indicates that this area has a significantly higher concentration of zinc compared to adjacent areas. The source of the zinc is not known.
- Arsenic was generally detected by pXRF analyses in amounts below the level of detection or in low concentrations. However, a couple of sample areas on the back and sinister surfaces had higher arsenic concentrations. Higher levels of arsenic are presumed to be derived from pigments in paint, known to be present on the Coronation Chair.
- Phosphorous was below the level of detection for most sample locations except the top and sinister surfaces. The cause of phosphorus concentration on these surfaces is not known.
- Several sample locations on the Stone of Destiny had elevated levels of chromium. It is suggested that locally elevated concentrations of chromium are related to the use of 20th-century tools for moving the Stone of Destiny in and out of the Coronation Chair.
- Discrete areas on the base and dexter surfaces show evidence of red and blue deposited material, respectively. The source of this deposited material is unknown, though it is likely that the blue material is minute traces of blue paint from 20th-century tools used to manoeuvre the Stone.

Endnotes

1 NJ Fortey, ER Phillips, AA McMillan and MAE Browne. 'A geological perspective on the Stone of Destiny'. *Scottish Journal of Geology*, 34(2) (November 1998), pp. 145-52.

2 SIEM-10: Kupferscheiefer, SIEM-02: Cordierite Gneiss, SIEM-06: Gabbro, SIEM-01: Granite, SIEM-05: Greywacke, SIEM-08: Melilite Basalt, SIEM-04: Nosean Phonolite, SIEM-03: Peridotite, SIEM-09: Siltstone, SIEM-07: Tonolite, GBW07103: Biotite granite (GSR-1), GBW07406: Soil (GSS-6), CS-M2: Bruker GeoExploration standard.

3 The question of whether or not the Stone of Destiny sandstone is calcareous has been unclear as previous investigators differ in their opinions (see Fortey et al., 1998).

4 David H Caldwell. Historic Environment Scotland, (2018). *Edinburgh Castle Research. The Stone of Destiny: Updating the scholarship,* states that "The dark patch on its upper surface is caused by a concentration of quartz-rich sandstone". Results of the analyses reported here do not support this conclusion.

DIGITAL DOCUMENTATION

Introduction

Prior to King Charles III's coronation, the Stone of Destiny and the Honours of Scotland (Crown, Sword of State and Sceptre) were digitised in 3D. The aims of the digitisation were to:

- produce digital imagery that could support the Applied Conservation Unit conserve the Stone of Destiny and Honours of Scotland.
- produce shareable content for public dissemination, which can provide an alternative way to virtually access the objects for those unable to visit in person or when they are not on display.
- create a 3D digital record of all the items to accurately capture their condition at the time of the survey.
- create a 1:1 scale 3D print replica of the Stone to aid the preparation for moving the Stone to Westminster, and to plan its insertion on the Coronation Chair.

The Digital Documentation and Innovation Team members conducting the documentation works for the Stone of Destiny and the Honours of Scotland were David Vacas Madrid, Sophia Mirashrafi, Adam Frost and Al Rawlinson.

3D digitisation

The Stone was removed from its showcase and placed onto three different supports (one for the main body and one for each handle) by a team of conservators.

The data capture was made using **photogrammetry**, a method to create accurate, measurable and texturized 3D models using photographs. The process consisted of taking photos during multiple loops at different heights (in ten-degree increments) around the object where the whole object fitted in the image. These images give the photogrammetry software context, which it uses for alignment. To these context photos, we add detail photos: the same capture was repeated multiple times, with new loops at different heights. We positioned the camera closer to the object each time to add resolution to the final **mesh** and texture of the model. The object was captured in this manner in four different positions (Figs 1-5), three with the handles open and one with the handles closed. The Stone was rotated into each position by two conservators.

In total, 862 photos were taken. The equipment used consisted of a full-frame DSLR camera (a Nikon D850) with a 35, 50 and 90mm lens (to take shots at different ranges). Because of the insufficient lighting in the room and the lack of space to install studio lighting, we opted for using a ring flash, a circular electronic flash tube that fits around a camera lens to provide medium-soft frontal lighting to the subject, with minimal shadow.

The camera settings chosen were an aperture of f/13, a shutter speed of 1/8sc and **ISO**-64. A high aperture allowed us to have the Stone in focus on all shots, while a low ISO allowed for better quality images with less **noise**. This is especially important when the photos will be used for photogrammetry, as the image noise can translat to defects on the 3D model. The downside of using a low ISO setting is that the camera sensor is less sensitive to light, so more lighting is needed on the scene. This was not an issue because we used a ring flash, enabling us to adjust the amount of light required. We also used a tripod and a remote shutter to avoid moving the camera during the shots and to get sharper images.

The Stone was also scanned with an Artec Space Spider **structured-light scanners** to provide additional geometry data.

We used six regular scales with **circular 20-bit targets** and a precision-calibrated scale with targets. These coded targets are detected automatically by the photogrammetry software and have a double function. On the one hand, they work as a valid match between images, helping the alignment during the photogrammetric process. On the other hand, they are essential for scale definition, allowing us to give a real-world scale to the 3D model. This scaling allowed us to measure any part of the object on the reconstructed model.

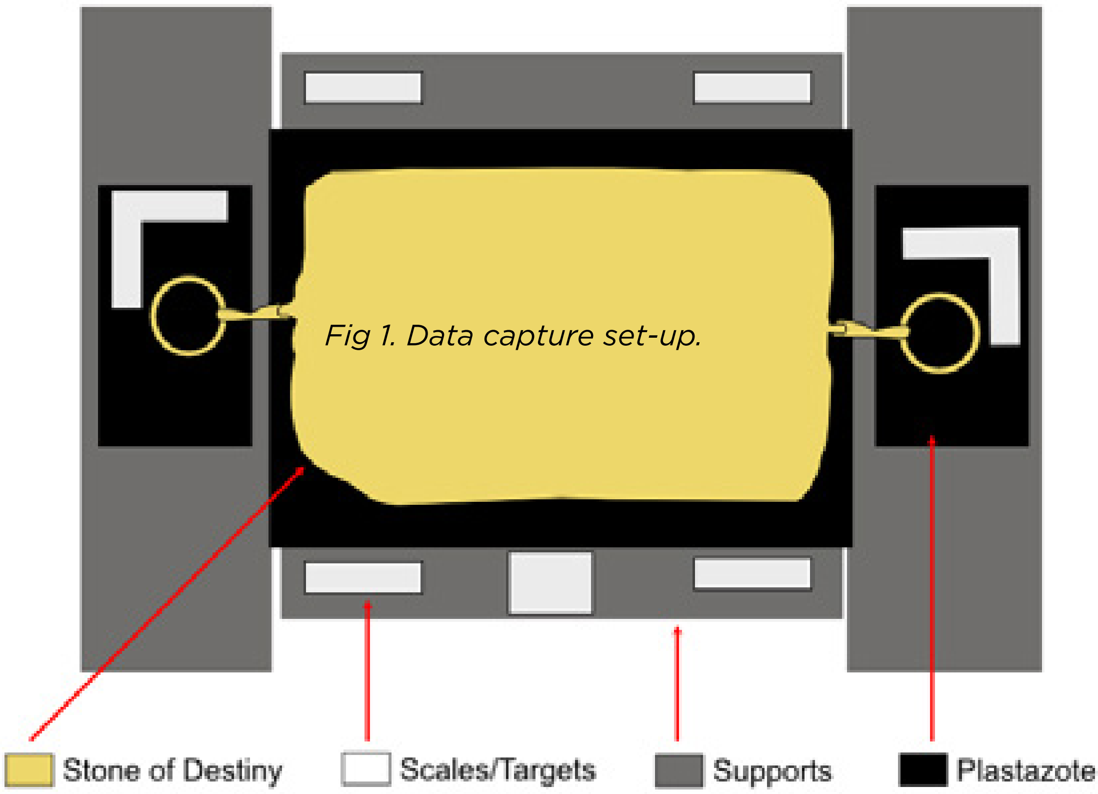

Fig 1. Data capture set up.

Fig 2

Fig 3

Fig 4

Fig 5

Figs 2-5. The data capture process for the various sides of the Stone of Destiny.

Pre-processing

All photos were taken in **RAW** format. A RAW file is the uncompressed and unprocessed image data captured by a digital camera. Shooting in RAW captures a high level of image detail with large file sizes and lossless quality. These images were edited, converted, and compressed in a non-destructive manner using Adobe Camera Raw, so that they could be used in photogrammetric software. We call this 'pre-processing'.

During this pre-processing, we also applied a colour management process to measure the accuracy of the colours reproduced by the camera and correct them to be as accurate a colour representation as possible. A colour profile was created using ColorChecker X-Rite, and **white balance** and tonal adjustment were corrected on Camera Raw. A ColorChecker chart, showing the colours at the time of capture, was also used on some of the images (Figs 6-9). It is important to note that the colour representation changes depending on the camera and lens used and, above all, by the lighting present during the capture.

We measure colours using two metrics, the **Delta-e** and the **Opto Electronic Conversion Function (OECF)**:

Delta-e

We analysed these metrics to estimate the difference between a sample colour, taken from our image, and a reference colour taken from a file (in CGATS format) that describes the colourimetry of our colour chart. Specifically, we use the CIE76 metric for the Delta-e, which is the oldest metric but the most commonly used. Below three Delta-e, the colour difference is not distinguishable by the human eye, so that should be our aim.

OECF

This metric evaluates if each zone of an image (highlights, half-lights and shadows) is in place. It allows us to make estimates about the relevance of the camera exposure and the presence of curves introduced during image processing, and to evaluate the neutrality or balance between the different RGB (redd-green-blue) channels. Unlike Delta-e evaluation, the OECF is only done on neutral patches.

The original colour chart taken during the capture has an average error 22.63 Delta-e, while the OECF was 52.5cv (Fig 8). After applying the colour management process, we get an average error of 7.52 Delta-e, and 7.83 cv for the OECF (Fig 9). The different lights in the room and the utilisation of flash are not the best source of light for light reproduction because the flash fluctuations, produced a not perfect colour reproduction, as our aim was a Delta-e below three and we get a Delta-e of 7.52. However, the colour management process significantly improved the colour reproduction from the 22.63 Delta-e on our original images.

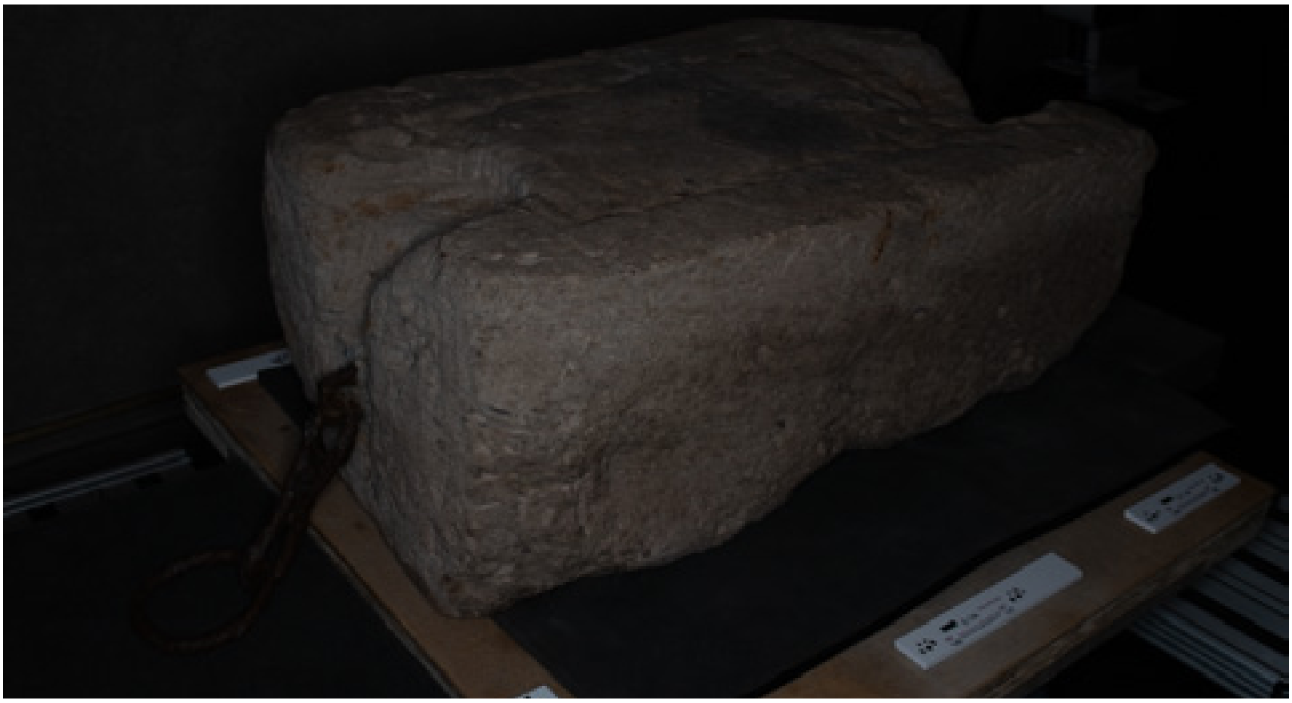

Fig 6. Before colour management.

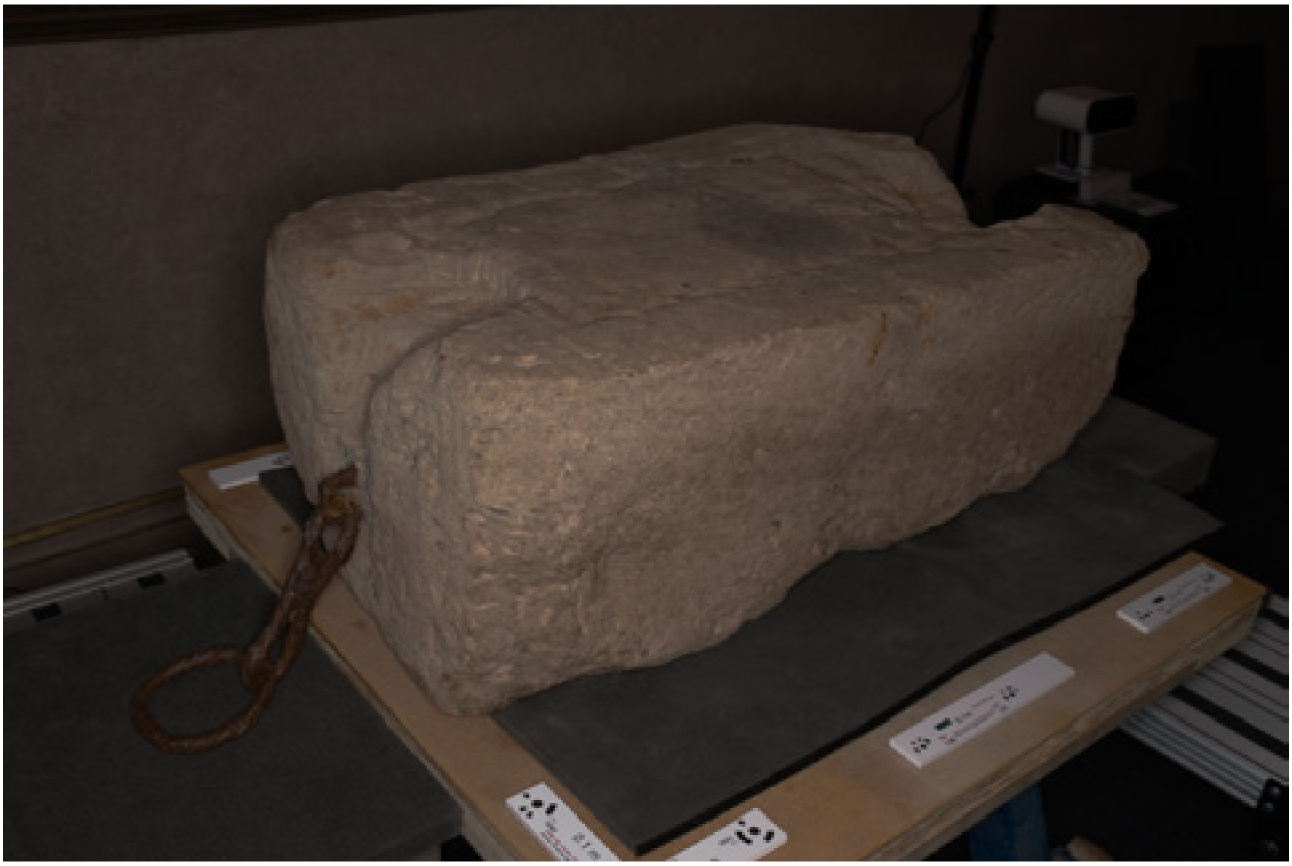

Fig 7. After colour management.

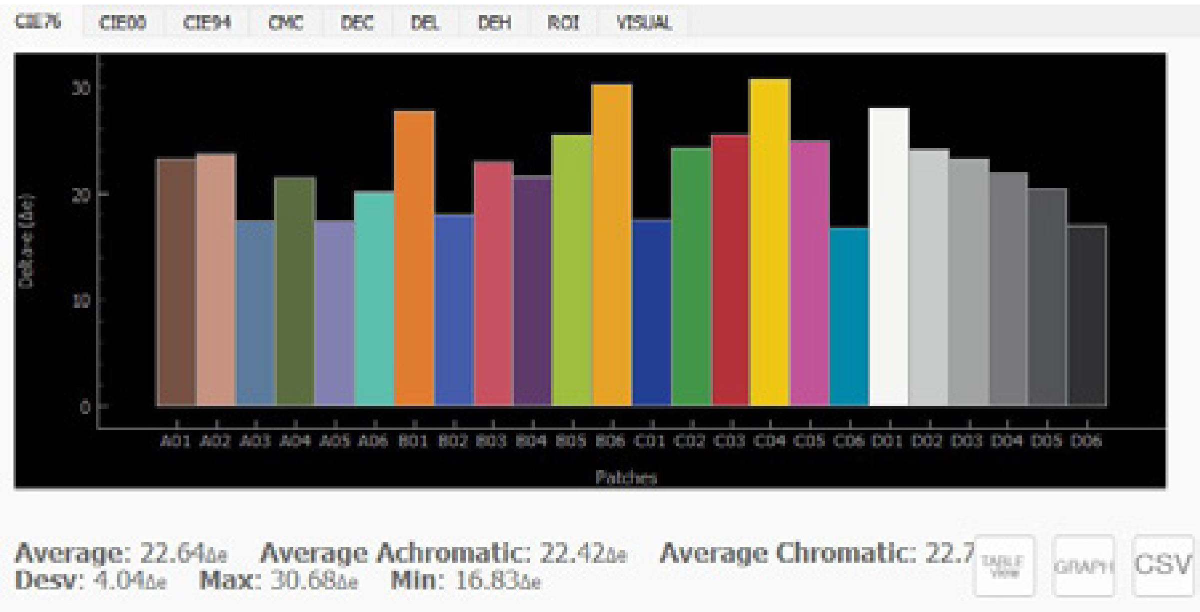

Fig 8a. Delta-e before colour management.

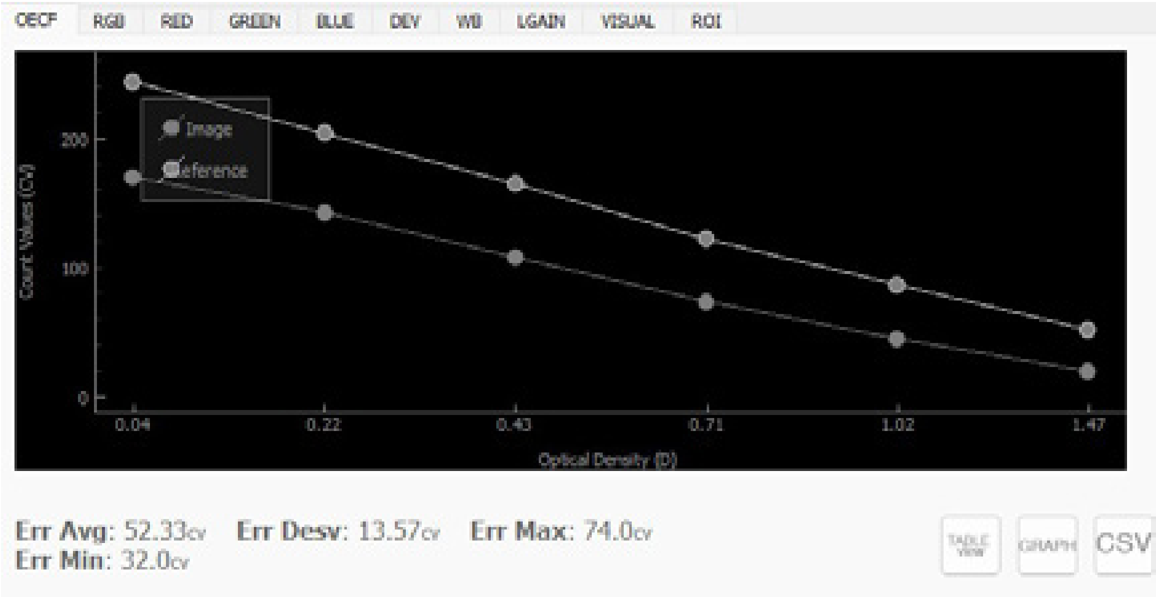

Fig 8b. OECF before colour management.

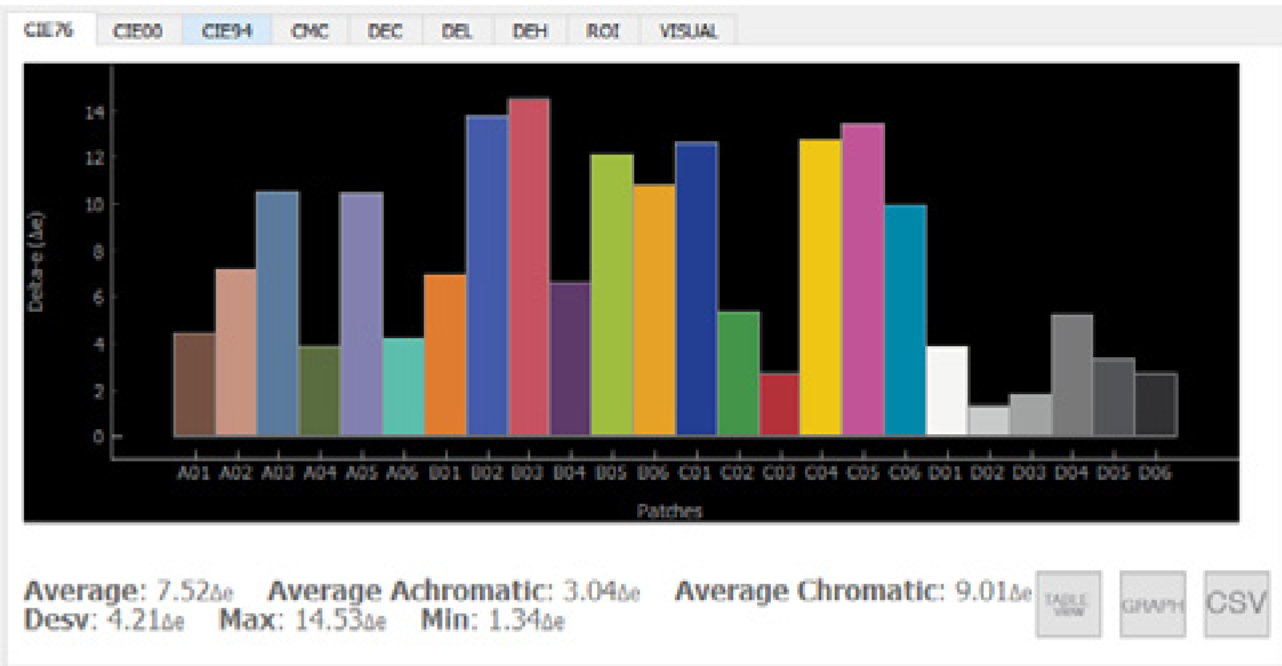

Fig 9a. Delta-e after colour management.

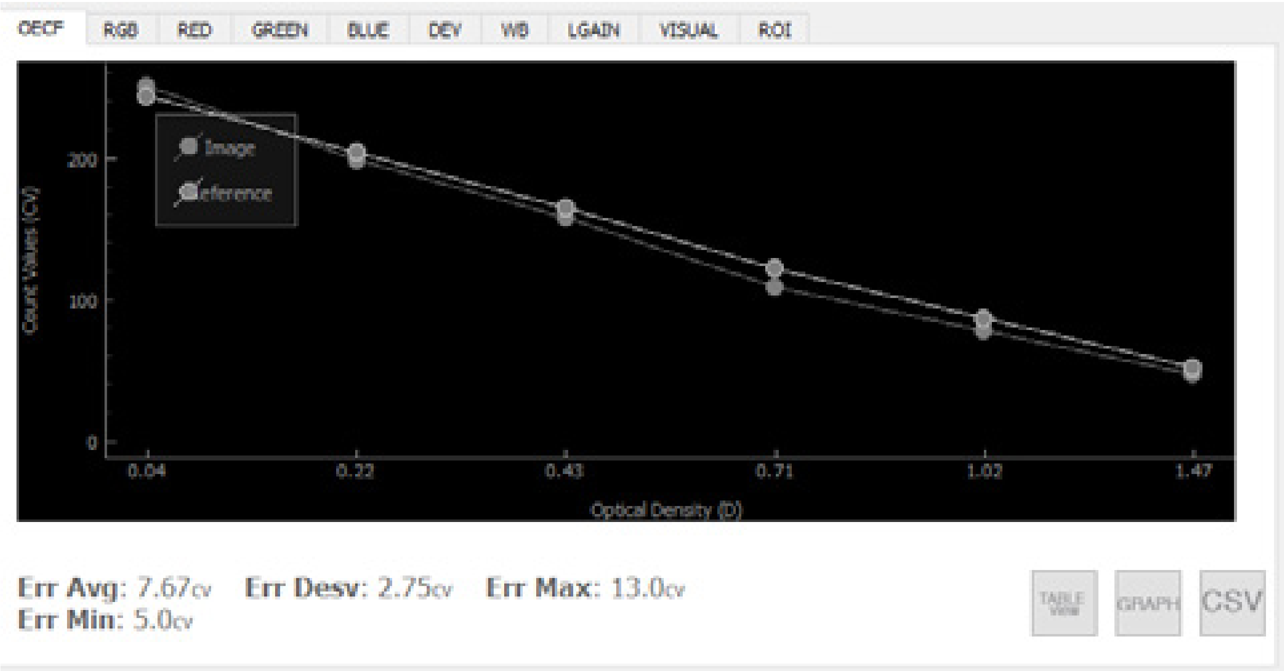

Fig 9b. OECF after colour management.

Processing

Once we have our images pre-processed and exported in TIFF format, we start processing in photogrammetry software, in this case **Reality Capture** (RC) (© Capturing Reality). During this process, we combine overlapping images (alignment) and calculate a polygon mesh and its texture.

We processed two different versions of the Stone. The first one (which will be referred to as version one) was intended to be a model with five different elements: the Stone itself and the handles (two elements per handle), producing an articulated replica. The second version (version two) was the Stone with the handles gathered on top of the Stone as it is usually positioned when it is on display. The workflow for both versions was the same:

1. Aligning each individual side (Table 1). The photogrammetric software calculates camera positions, orientations and internal camera states for every input image. If the data capture has been done correctly, all the photos will be aligned, creating a visual point cloud that represents the object.
2. Detecting markers (April Tags 16h5 and Circular 20-bit targets) and scaling using the precision targets. See '3D digitisation' above for fuller explanation of these targets.
3. Re-aligning using applied scale.
4. Creating a normal detail mesh. Once camera poses are known, the software can calculate a completely dense 3D mesh of the preferred quality. The result is a very dense triangular mesh.
5. Filtering all elements outside the object and exporting **masks**. For version one, the Stone and the handles were reconstructed separately. To do that, the four parts

of the handles and the Stone were masked and exported individually, one each time. Masking was essential to combining the different sides of the Stone. It created a black (unmasked areas) and white (masked areas) PNG file associated with each TIFF and allowed us to do the processing when we needed to turn the Stone on its side, upside down.

6. Importing the masks back and processing a new clean alignment without external elements, creating a new project for each element.
7. Exporting components for each side.
8. Creating a new RC project, importing the components and doing a new alignment (Fig 10).
9. Scaling.
10. Creating a high-detail mesh.
11. Texturing (Table 2). Texturing consists of two steps: **unwrapping,** and texture image colour calculation. UV unwrapping is a projection of a 3D model surface as 2D information. After this UV map is created at the desired resolution (8K in this case), the images are projected, resulting in a photorealistic texture.

Table 1: Alignment settings on Reality Capture.

Feature	**Setting**
Alignment engine	RealityCapture
Alignment mode	High
Max features per mpx	10000
Max features per image	40000
Detector sensitivity	Medium
Preselector features	20000
Image downscale factor	1
Max feature reprojection error	1.000000
Use camera positions	Yes
Lens distortion model	Brown4 with tangential2
Final optimization	Yes

Table 2: Texturing settings on Reality Capture.

Feature	Setting
Colouring style	Texturing-based
Unwrapping style	Adaptive texel size
Count of textures	11
Texture resolution	8192 x 8192
Chart gutter size	3 texels
Texture utilisation (with gutter)	85%
Optimal texel size	0.000061 units per texel
Minimal texel size	0.000061 units per texel
Maximal texel size	0.000061 units per texel

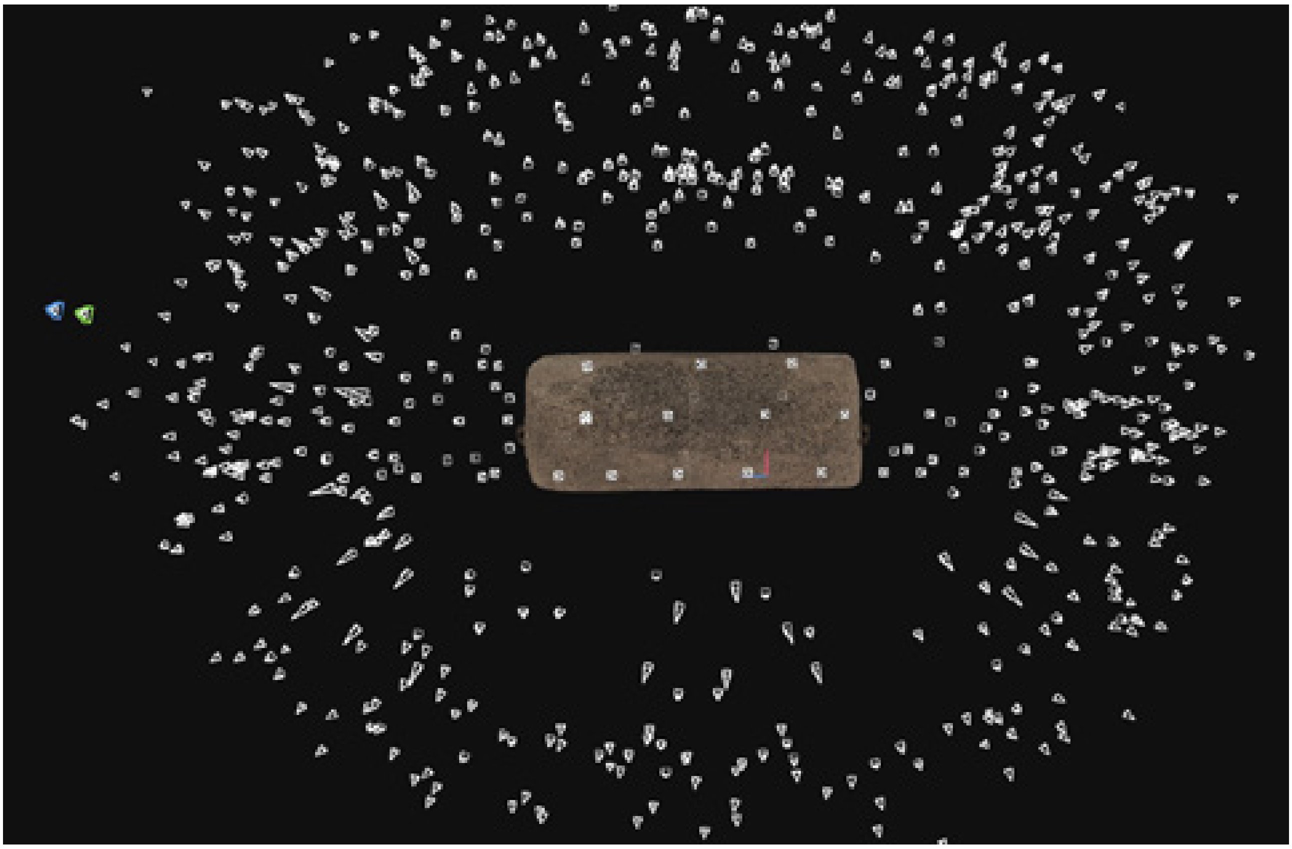

Fig 10. Combined alignment for version one.

Fig 11. Handle A. Piece one.

Fig 12. Handle A. Piece two.

Fig 13. Handle B. Piece one.

Fig 14. Handle B. Piece two.

Post-processing

Post-processing refers to any edits made to the 3D model obtained from the photogrammetric software. These edits are sometimes necessary to fix issues that the photogrammetry is not able to reconstruct, such as holes in areas where we don't have images or noise or irregularities on a 3D surface, usually produced by reflective materials.

Cleaning noise

The 3D model of the Stone itself did not need any editing. Noise was only present on the handles, which are made of a slightly reflective material. The workflow used consisted of simplifying the level of detail of the model (known as **decimating**), subdividing the amount of polygons and projecting detail back. After this, some manual work was done, especially on the interior of the handles, using different brushes to flatten the surfaces where the noise was deforming the geometry (Figs 15 and 16).

Closing holes

Some small areas on the rings of the handles were obscured in all images, and all the positions the Stone was captured in. To close these holes, we applied a remeshing on Zbrush using the Dynamesh tool and sculpting the shape back (Figs 17 ansd 18).

The mesh where the handles were placed on top of the Stone presented some extraneous geometry created by the software to close the gaps in the obscured areas. This creating a bridge of geometry that we removed on Zbrush (Figs 19-22). The edited models were imported back to Reality Capture, where they were **texturised**.

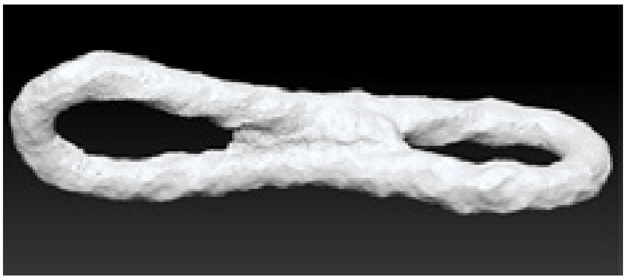

Fig 15. Handle before editing.

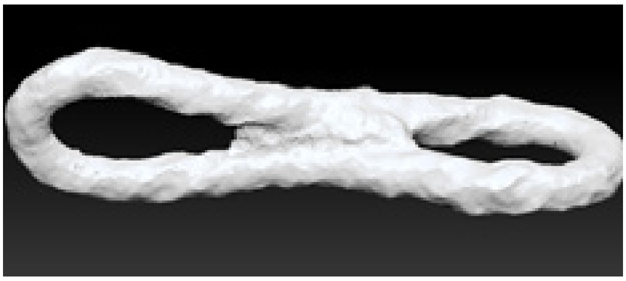

Fig 16. Handle after editing.

Fig 17. Handle A after closing holes.

Fig 18. Handle B after closing holes.

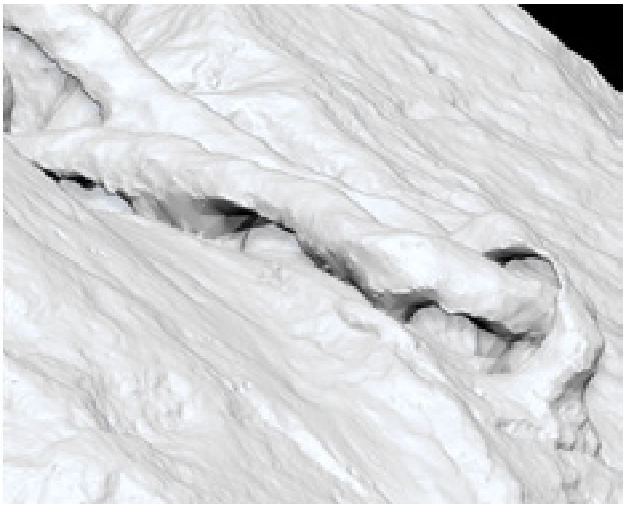

Fig 19. Version two before editing (sinister side).

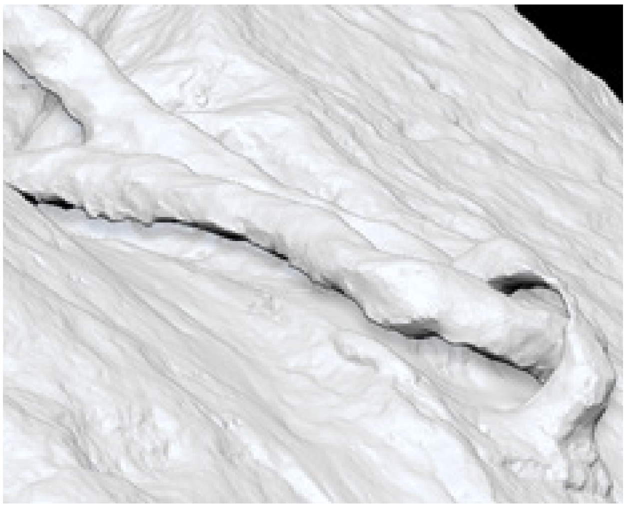

Fig 20. Version two after editing (sinister side).

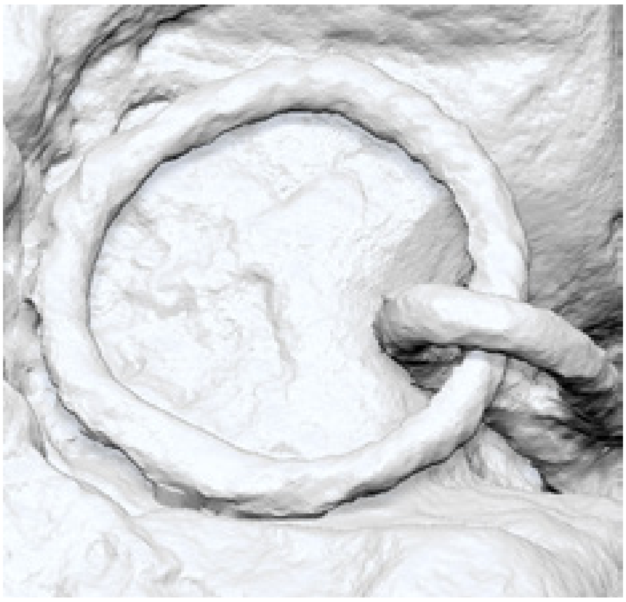

Fig 21. Version two before editing. Dexter face socket.

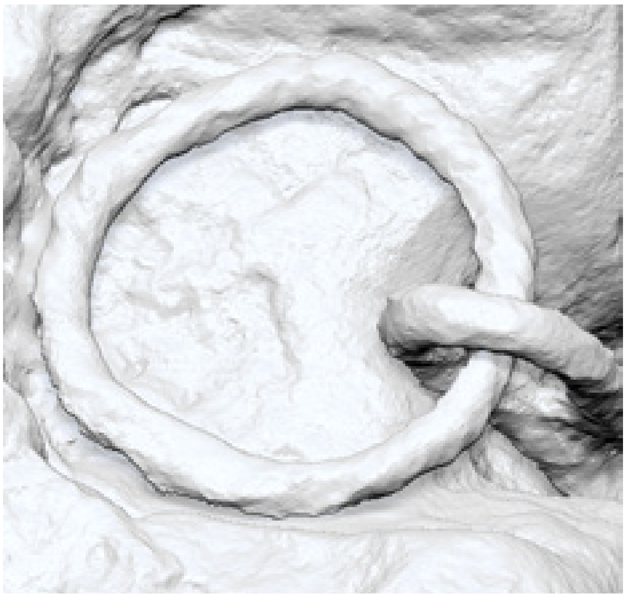

Fig 22. Version two after editing. Dexter face socket.

Other than the edited mesh, a 3D print-ready mesh and an optimised mesh for web visualisation were created for each of the two versions:

- **3D Print.** The Stone was decimated to 7.2 million polygons and imported to Meshmixer to analyse and correct any issues that the geometry could have. It was then exported as an **STL** file, ready for 3D printing. The four parts of the handles were also decimated and processed on Meshmixer before exporting their STL versions.
- **Web.** The web version was decimated from the edited version to obtain a mesh of around 228K polygons, with a smaller unwrap of just one texture, and the **normals** from the edited version projected onto it. The elements of the handles were also decimated with a texture of 4K definition each.

Outputs

- **RAW.** Original mesh. Texturised. No editions.
- **Edited**. Decimated version, edited. Noise removed and issues on the mesh fixed. Texturised.
- **3D Print.** Watertight mesh optimised for 3D printing.
- **Web.** Optimised version. Diffuse and normal maps were projected on one 8K map. The optimised model can be viewed on Sketchfab: https://sketchfab.com/3d-models/stone-of-destiny-edinburgh-castle-4d46d1df627d41a2adc65f6550b2fa9c.

Other outputs

- **Renders.** Eight with different views.
- **Orthoviews.** 24 orthoviews (interior, exterior and sections) were produced in high-resolution (15360x8640). For easier use, all the orthoviews were grouped on PDF sheets (four pages) with two different resolutions (A0 and A4). The PDF sheets have the object information and scale reference (Figs 23 and 24).

- **Animation.** 2591 frames (3840x2160) rendered to produce an animation of 1 minute 43 seconds, 60 frames per second. Two versions of the same animation were exported: one with a black background and one with a gradient background and the HES logo (Fig 25).

Fig 23. PDF sheet example: orthoviews.

Fig 24. PDF sheet example: different views of incision numbers and are where they are found.

Conclusions

The 3D digitisation work undertaken by the Digital Documentation and Innovation Team was the most detailed documentation of the Stone of Destiny ever undertaken. It has provided accurate 3D imagery and models that will prove useful for future conservation and research activity, and as a digital record of the Stone.

This report will also act as a record of the digital documentation process and the considerations that go into it, as a guide to others involved or interested in this type of work. It reflects on lessons learned and identifies areas for improvement in future practice.

Fig 25. Render on a gradient background with HES logo.

REPORT CONCLUSIONS

The condition assessment, scientific analysis and digital documentation work carried out on the Stone of Destiny in preparation for the coronation of King Charles III in 2023 has provided vital insights into the Stone and its continued conservation.

The condition assessment led to new discoveries about the Stone, including a previously unreported incised inscription of Roman numerals or letters, possibly part of an accession system, and an incision resembling the letter 'H'. The assessment report highlights the importance of condition assessments and why they are vital in object conservation as they:

- create a record of an object than can be used as a reference when monitoring changes over time, thus informing conservation decision-making; and
- enable conservators to spot any issues they need to investigate, allowing them to react in a timely manner.

Signs of ageing such as previous repairs starting to fail, and natural issues within the material of the Stone such as fine cracks and flaking were identified and treated. Recommendations were provided for any future conservators required to assess, treat, or move the Stone in the future.

Scientific analysis of the Stone provided rich data about the its composition, and pXRF analysis revealed how the Stone has been affected by its environments in the past: the gypsum on the stone was likely due to the presence of sulphate and calcium oxide from surface contamination (like pollution for example); traces of arsenic were likely from pigments in paints known to be on the Coronation Chair; and concentrations of chromium, and minute traces of blue paint, were probably from 20th-centry tools when the Stone had to be moved. This data can be used to inform appropriate treatments, maintenance methods, and environment for the Stone.

Finally, the process of digitally documenting the Stone of Destiny has created a reference resource which may be of use to other heritage organisations or conservators producing 3D digital records of their own collections objects. It catalogued lessons learned and key considerations when working with fragile and precious objects and how to produce a high-quality 3D model. This model can be used as a digital record, can provide an alternative to physical access to the stone for research and conservation purposes, and can offer a learning and outreach resource accessible to audiences worldwide.

GLOSSARY

Accession number/system – a number assigned to a record or item for cataloguing within a collection or database.

Accretion – the gradual accumulation of additional layers or matter.

Acrylic – a synthetic resin made from polymers of acrylic acid.

Aggregate component – an element, particle or fragment forming part of a loosely compacted material or structure.

Articulated (iron ring) - having two or more sections connected by a flexible joint.

Calcareous – containing calcium carbonate.

Calcium carbonate – a white slightly soluble solid occurring naturally as calcite within chalk, limestone and marble.

Calcium oxide – a white caustic alkaline solid.

Cementitious – having the properties of cement.

Circular 20-bit targets - a circular target with a 20-bit data ring. The circle is divided into 20 parts. This kind of target is recognized automatically by photogrammetric software, helping with the image's alignment

Cuprous – of or containing copper.

Decimating (model) - simplifying the level of detail of the model.

Delta-e – a standard measurement created by the Commission Internationale de l'Eclairage (International Commission on Illumination) that quantifies the difference between a sample colour and a reference colour.

Deposit – a layer or mass of accumulated matter.

Dexter – a convention sometimes used in collections management/applied conservation denoting the right side of an object from its perspective.

Dissolution – dissolving or being dissolved.

Grains – small hard particle or crystal of stone, typically visible only when a surface is magnified.

Gypsum – a soft, grey or white mineral. A hydrated form of calcium sulphate.

In situ – situated in its original place.

Intergranular material – materials or substances existing between individual grains.

ISO – a number that represents a camera sensor's sensitivity to light. Can be used to brighten or darken an image.

Litharenite – sandstones with a significant (>5%) component of lithic fragments.

Lithic fragments – rock fragments contained within a subsequently formed rock.

Lower Devonian sandstone – formed during the Devonian geological period.

Magnetic susceptibility – a measure of how much a material will become magnetised in an applied magnetic field.

Masks – a non-destructive way to hide parts of an image or layer without erasing them. Using masks on photogrammetry helps to filter-out unwanted geometry during the reconstruction phase.

Mesh – polygonal geometry generated directly from point cloud data.

Mica – a shiny, laminated silicate mineral found in some rocks.

Mineralogically immature – containing a high relative proportion of less stable minerals (i.e., lithic fragments, feldspar) relative to resilient minerals (i.e., quartz).

Noise – any unwanted detail on a 3D mesh. This includes tiny imperfections or random artefacts which aren't present on the real object. Noise appears typically on shiny and reflective surfaces, as the photogrammetry software struggles to interpretate the mesh.

Normals - other texture files (not the 3D model) where each pixel represents the difference in direction the surface should appear to be facing, allowing for the use of less geometry.

Opto electronic conversion function (OECF) – a metric used in digital documentation pre-processing to evaluate whether each highlight and shadow of an image is in place.

Orthoview – a representation of a three-dimensional object in two dimensions. Orthoviews or orthophotos are geometrically corrected and can be used to take true measurements.

Petrographic analysis – an analysis of the properties of rocks, including grain size, texture, and colour, by examining thin sections.

Photogrammetry – or SfM photogrammetry, is a technique that allows the reconstruction of accurate 3D models from overlapping successive photographs taken from cameras at various angles. These 3D models can contain scale and texture information.

Photomicrograph - a photograph of a microscopic object, taken with the aid of a microscope.

Portable X-ray fluorescence - a non-destructive analytical technique used to determine the elemental composition of materials.

RAW format – files containing uncompressed and unprocessed image data.

Reality Capture © – photogrammetry software used for creating 3D models.

Retopology - the process of modifying or optimising the polygonal mesh of a 3D model.

Scone Formation sandstones – sandstones from the early Devonian geological period, often found between Dundee, Arbroath, Blairgowrie, and Scone.

Sinister - a convention used in collections management/applied conservation denoting the left side of an object from its perspective.

STL file - a 3D format, typically used for 3D printing.

Structured-light scanning – a device/method for recording the three-dimensional shape of an object using projected light patterns and a camera system.

Texturing (models) – a technique for adding surface detail and colour to a 3D model to give the look of a textured and detailed surface to 2D pictures that are mapped onto the surface of a 3D object.

Tonal adjustment – Tonality refers to the range and distribution of tones and the smoothness of gradation between them. Tonal adjustment is necessary for a correct reproduction of colour.

Unwrapping (models) – ‘flattening’ a 3D model into a 2D image so that it can be wrapped with a texture.

Weathering – when a material is altered or deteriorates due to consistent exposure to certain elements or conditions, such as wind, rain, or heat.

White balance – the colour temperature at which white objects on an image appear white. All the colours in a photo are determined by how the white balance is set. For accurate white balance reproduction, a grey chart is used as a reference.

FURTHER READING

‘A geological perspective on the Stone of Destiny’. NJ Fortey, ER Phillips, AA McMillan, and MAE Browne. Scottish Journal of Geology, 34(2), 145-52, (November 1998).

‘A summary of ultra-violet fluorescent materials relevant to conservation’. Danielle Measday; Briony Pemberton and Charlotte Walker. AICCM National Newsletter, no. 137, Australian Institute for the Conservation of Cultural Material, (March 2017).

Edinburgh Castle research. The Stone of Destiny: updating the scholarship. David H. Caldwell. Historic Environment Scotland (Edinburgh, 2018).

Edinburgh Castle: statements of significance. Historic Environment Scotland (Edinburgh, 2024).

Research shines new light on the Stone of Destiny. Reed Hudson. Historic Environment Scotland (April 2023).

Scotland’s Stone of Destiny. Nick Aitchison. The History Press (2009).

Short Guide 13: Applied digital documentation in the historic environment. Adam Frost. Historic Environment Scotland (Edinburgh 2018).

Stone of Destiny conservation assessment. Christa Gerdwilker. Historic Environment Scotland (Edinburgh, 2016).

The Coronation Chair and Stone of Scone: history, archaeology and conservation. W. Rodwell. Oxbow Books (Oxford, 2013).

The Stone of Destiny, symbol of nationhood. D. Breeze and G. Munro. Historic Environment Scotland (Edinburgh, 1997).

The students who stole the Stone of Destiny. Steve Brocklehurst. BBC News (March 2023).

HISTORIC ENVIRONMENT SCOTLAND | ÀRAINNEACHD EACHDRAIDHEIL ALBA

Historic Environment Scotland
Longmore House, Salisbury Place
Edinburgh EH9 1SH
0131 668 8600
historicenvironment.scot
Historic Environment Scotland – Scottish Charity No. SC045925
Registered Address: Longmore House, Salisbury Place, Edinburgh EH9 1SH